THE PENNSYLVANIA STATE UNIVERSITY
SCHREYER HONORS COLLEGE

DEPARTMENT OF MATERIALS SCIENCE AND ENGINEERING

THERMODYNAMIC MODELING AND FIRST-PRINCIPLES CALCULATIONS OF THE CR-HF-Y TERNARY SYSTEM

BRADLEY HASEK
Spring 2010

A thesis
submitted in partial fulfillment
of the requirements
for a baccalaureate degree
in Materials Science and Engineering
with honors in Materials Science and Engineering

Reviewed and approved* by the following:

Zi-Kui Liu
Professor of Materials Science and Engineering
Thesis Supervisor

Paul R. Howell
Professor of Metallurgy
Honors Adviser

* Signatures are on file in the Schreyer Honors College.

ABSTRACT

This thesis describes the thermodynamic modeling of the ternary Cr-Hf-Y system. Chromium, hafnium, and yttrium are all used as alloying elements in nickel superalloys. Nickel superalloys usually contain many different alloying elements, so there becomes a need to understand the phase equilibria of large, multicomponent systems. This can be accomplished by using the CALPHAD method of modeling. CALPHAD modeling requires experimental data to better model the system. In the absence of experimental data, first-principles calculations can be used to predict thermochemical data.

Before modeling the Cr-Hf-Y system, the binary Cr-Hf, Cr-Y, and Hf-Y systems must be modeled. In the Cr-Y and Hf-Y system, there is limited experimental data, so first-principles calculations are done on the BCC and HCP solid solution phases using special quasirandom structures (SQS's) to model the disordered systems. The symmetry is also investigated to ensure symmetry is not lost during relaxation. Using the first-principles calculations, the enthalpy of mixing is used to model these systems. The Cr-Hf system is modeled with experimental data and with first-principles calculations done on the Laves phase. With the three binary systems modeled, the ternary system is then modeled without any experimental data present. Isothermal sections are presented from 1273 K to 2200 K.

TABLE OF CONTENTS

LIST OF FIGURES

LIST OF TABLES

ACKNOWLEDGEMENTS

I would like to thank the following people for all their help:

- Dr Zi-Kui Liu for giving me the opportunity to truly understand the power of thermodynamics
- All the members of Phases Research Lab for their support and guidance

Chapter 1

Introduction

1.1: Nickel Superalloys

Nickel superalloys have a very diverse set of applications. Not only do they maintain high strength at high temperatures, but they are also highly resistant to oxidation, carburization, sulfidation, and nitriding. For aerospace applications, the ability to endure under even higher temperatures and maintain their properties longer is an ongoing goal. To achieve these goals, the addition of more and more alloying elements, such as chromium, hafnium, and yttrium, may be necessary, creating large, multicomponent systems. As more alloying elements are added, it becomes critical to understand the phase stability in multicomponent nickel-based systems.

1.2: Objectives

Alloy design is usually a very tedious process. It can be time-consuming and also expensive, as it requires small test alloys be processed from melt through some defined processing route. One thing that is examined is the presence of any undesirable phases. This information is critical to the properties of the alloy. One way to investigate phase stability is by the CALPHAD method, which is described in detail in the next chapter.

There are many benefits to using modeling in lieu of traditional alloy design. There is a cost associated with processing many samples that can be reduced if a modeling approach is taken. There are also environmental issues that can be addressed. While alloy processing has taken great strides to become less of an environmental hazard, the reality is that the environment

is still affected by it. With a reduction in test samples also comes a reduction in many forms of pollution.

Other advantages of modeling include the ability to create materials that have less exotic alloying elements. This can be beneficial in a number of ways. The material may be more sustainable if it can be made from more prevalent materials and from materials that can more easily be recycled. There is also the possibility to eliminate the need to get raw materials that may come from unethical business practices, such as the environmental destruction of third-world countries. It may also eliminate the need for any unsafe raw material use.

In modeling a large, multicomponent system, the smaller systems must be modeled first. Binary systems are combined into ternary systems; ternary systems are combined into quaternary systems, and so on. The goal of this thesis is to model the Cr-Hf-Y ternary system by first modeling the three constituent binary systems. Once the ternary system has been modeled, it can be incorporated into a much larger nickel superalloy database.

.

1.3: Outline

This thesis will consist of seven chapters. Chapter 2 will provide a description of each of the methods used, including CALPHAD modeling and first-principles calculations. In Chapter 3, Chapter 4, and Chapter 5, the modeling of Hf-Y, Cr-Y, and Cr-Hf will be examined, as well as published data and first-principles calculations. Chapter 6 will discuss the combination of the three binary systems to create the Cr-Hf-Y ternary system. Chapter 7 concludes this thesis and also suggests future work.

Chapter 2

Computational Methodology

2.1: Introduction

The goal of this thesis is to understand the phase equilibria of the Cr-Hf-Y ternary system by way of the CALPHAD (Computer Coupling of Phase Diagrams and Thermochemistry) method. This method involves describing the Gibbs energy function of individual phases as a function of temperature, pressure, and composition. To help determine specific parameters that describe the Gibbs energy, experimental data is put into the model. In the absence of experimental data, first-principles calculations have been shown to adequately predict thermochemical properties of phases. First-principles calculations are based on density functional theory. This is useful in systems with little experimental data and also in metastable regions. Phase equilibria of the Cr-Hf-Y system can be determined by modeling the three binary systems and combining them to create the ternary system. In this chapter, underlying principles of thermodynamic modeling and first-principles calculations will be given, as well as details of the calculations performed in this work.

.

2.2: Density Functional Theory

Phase equilibria data is far more abundant in literature than thermochemical data for individual phases. While a system can be reproduced solely with phase equilibria data, the model may not be unique, as the stability of phases is related to the relative values of Gibbs energy. To

get a more accurate description of the Gibbs energy, thermochemical data should be used, as it only depends on one phase, not the relationship between two phases. This data is far less available, however, and may need to be predicted by density functional theory.

Density functional theory utilizes the concepts of quantum mechanical electronic theory to determine the total energy of a crystalline solid simply by inputting the atomic coordinates and the atomic species. These calculations are referred to as first-principle calculations because they are performed "from the beginning" meaning there is no experimental data required to perform them. This freedom from experimental observations allows for calculations to be done on phases that have not yet been experimental verified.

The term density functional theory originates from the fact that the energy calculated is a function of the charge density of electrons in a solid. The time-independent Schrödinger Equation can only describe a single particle at one specific time. The system is defined by the wavefunction at that time, and from this wavefunction, the total energy can be calculated. This equation can be written as

$$\text{Eq. 2.1:} \qquad \hat{\boldsymbol{H}}\boldsymbol{\Psi} = \boldsymbol{E}\boldsymbol{\Psi}$$

where $\hat{H}$ is the Hamiltonian operator, Ψ is the wavefunction, and E is the energy of the system. The use of this equation is limited to only one electron. Attempting to solve this problem for the number of electrons in even a single primitive cell cannot be done. It is because of this that a method was developed to describe the density of electrons rather than the wavefunction itself[1, 2]. This assumes that the density uniquely defines the wavefunction as well as the properties of the system. This means, then, that the total energy can be written as

$$\text{Eq. 2.2:} \qquad \boldsymbol{E_T} = \boldsymbol{E}[\boldsymbol{\rho}(\vec{\boldsymbol{r}})]$$

where $\boldsymbol{\rho}(\vec{\boldsymbol{r}})$ is the density of electrons and the groundstate of the system is found by minimizing $\boldsymbol{E_T}$. The energy of the system is the sum of several parts:

$$\text{Eq. 2.3} \qquad \boldsymbol{E}[\boldsymbol{\rho}] = \boldsymbol{T_0}[\boldsymbol{\rho}] + \boldsymbol{V_{ext}}[\boldsymbol{\rho}] + \boldsymbol{V_{Hartree}}[\boldsymbol{\rho}] + \boldsymbol{E_{xc}}[\boldsymbol{\rho}]$$

where $\boldsymbol{T_0}$ is the kinetic energy of the electrons without interactions, $\boldsymbol{V_{ext}}$ is the potential energy of the ions interacting with the electrons, $\boldsymbol{V_{Hartree}}$ is the Coulombic interaction between a single electron with the rest of the system. The final term,$\boldsymbol{E_{xc}}$, is the exchange and correlation energy which includes many complex interactions, such as all the electrons interacting with each other.

The form of $\boldsymbol{E_{xc}}$ is unknown, so approximations are used, such as the local density approximation (LDA)[3] and the generalized gradient approximation (GGA)[4]. LDA assumes the exchange correlation is only a functional of local density of electrons, whereas GGA also considers the gradient of charge density. Results using GGA are generally in better agreement with experimental data than results using LDA.

The total energy cannot be included into CALPHAD modeling because the energy has no reference state. The enthalpy of mixing, however, can be used because the reference states are the pure elements of the same phase. Pure elements and solid solution energies can all be calculated from first-principles and the enthalpy of mixing can be calculated by the following equation:

Eq. 2.4 $$\mathbf{\Delta H_{mix}(A_iB_j) = E(A_iB_j) - x_aE(A) - x_bE(B)}$$

where $\mathbf{\Delta H_{mix}(A_iB_j)}$ is the enthalpy of mixing for the solid solution and $\mathbf{E(A_iB_j)}$, $\mathbf{E(A)}$ and $\mathbf{E(B)}$ are the energies of the solid solution, pure A and pure B, respectively from first-principles.

.

2.3: Disordered Phases and Special Quasirandom Structures

First-principles calculations work well because a relatively small number of repeating atoms are able to represent the repeating crystalline nature of most solids by applying periodic boundary conditions. This becomes complicated when trying to calculate the total energy of a

disordered phase, such as a substitutional solid solution. There are three main approaches to attempt to simulate the random configurations:

1) The Supercell method requires very large supercells, on the order of hundreds of atoms, to reproduce the interactions of a truly random structure. This method is computationally very time-consuming.
2) The Coherent Potential Approximation (CPA) method [5] is constructed from the assumption that the average scattering of electrons off the alloy components should disappear[6]. This method does not consider local relaxations and the effects of alloying on the distribution of local environments cannot be taken into account. Local relaxations have been shown to significantly affect the properties of random solutions[7], especially when the atoms vary in size and, therefore, their omission is a major disadvantage.
3) The Cluster Expansion method[8] determines the energy of any random alloy by considering the energies of many different configurations. It requires calculations of tens of ordered structures and, as with the supercell method, is very time-consuming.

Each of these techniques has limitations, such as required computing power or accuracy. Special Quasirandom Structures (SQS) was developed by Zunger et al.[9]. It has the advantage of being able to accurately mimic the interactions of random solutions with only a few atoms, usually between 4 and 32 atoms, while saving time. As the atoms relax, they locally disturb the structure away from equilibrium, providing the local relaxation that was shown to be significant.

The ordered structure used for an SQS should have similar interaction as a random solid. Interactions between nearest neighbors contribute more to the total energy than distant neighbors do. In binary systems, each site, *i*, is assigned a spin variable of – 1 if the site is occupied by A atoms and + 1 if the site is occupied by B atoms. Sites are grouped into "figures" f=(k,m), where

k=1,2,3… representing points, pairs, triplets of atoms and so on of the mth nearest neighbor. The correlation functions, $\overline{\Pi}_{k,m}$, are the averages of the products of the spin variables of figure k at distance m. The optimum SQS is one that best satisfies the condition:

Eq. 2.5: $$\left(\overline{\boldsymbol{\Pi}}_{\boldsymbol{k,m}}\right)_{\boldsymbol{SQS}} \cong \left(\overline{\boldsymbol{\Pi}}_{\boldsymbol{k,m}}\right)_{\boldsymbol{R}}$$

where $\left(\overline{\boldsymbol{\Pi}}_{\boldsymbol{k,m}}\right)_{\boldsymbol{SQS}}$ is the correlation function of the SQS and $\left(\overline{\boldsymbol{\Pi}}_{\boldsymbol{k,m}}\right)_{\boldsymbol{R}}$ is the correlation function of a random alloy.

2.4: Relaxations and Radial Distribution Analysis

After relaxations are performed on the various phases, it is important to determine whether symmetry was preserved. Relaxations should be performed with the initial symmetry in mind. Consideration should be given to how many degrees of freedom the initial structure has. In some cases, local relaxations in SQS's may become so large that the symmetry of the original structure may be lost. If this is found to be the case then limiting the relaxation can be considered to allow the relaxed structure to correspond to the parent lattice. This is necessary because modeling requires a description of the phase even where it is not stable. Even though local relaxations may be slightly altered by this, it can still be considered a reasonable calculation.

To determine the symmetry of a structure, a radial distribution (RD) analysis was used. In this analysis, it can be shown the relative number of nearest neighbors to an atom. By comparing the ideal structure to the different relaxation methods, an idea into how well the symmetry was maintained can be achieved.

2.5: CALPHAD Modeling

The Gibbs energy contains an enthalpy and an entropy term as follows:

$$G = H - TS \quad \text{Eq. 2.6:}$$

and the polynomial of the molar Gibbs energy as a function of temperature is usually expressed as:

$$G_m - H_m^{SER} = a + bT + cTlnT + dT^2 + eT^3 + fT^{-1} \quad \text{Eq. 2.7:}$$

where H^{SER} is the molar enthalpy of the phase at 298.15 K and 1 atm, which is also known as the stable element reference (SER) by Scientific Group Thermodata Europe (SGTE) and a, b, c, d, e and f are all fitting parameters. Eq. 2.7 works well when lots of data is present.

For binary phases, the Gibbs energy functions are slightly different. Two types of phases present in binary systems are solution phases and stoichiometric compounds, also known as line compounds. The Gibbs energy formalism for a one-sublattice, substitutional solution model is as follow:

$$G_m = G_m^o + \Delta G_{mix}^{ideal} + \Delta G_{mix}^{xs} \quad \text{Eq. 2.8:}$$

where G_m^o is the mechanical mixing term of elements A and B given by the equation:

$$G_m^o = x_A G_A^o + x_B G_B^o \quad \text{Eq. 2.9:}$$

ΔG_{mix}^{ideal} is the interaction between elements assuming a random mixture, which can be written as:

$$\Delta G_{mix}^{ideal} = RT(x_A lnx_A + x_B lnx_B) \quad \text{Eq. 2.10:}$$

and ΔG_{mix}^{xs} is the deviation from the ideal solution behavior. This can be characterized by the Redlich-Kister polynomial[10]:

Eq. 2.11: $$\Delta G_{mix}^{xs} = x_A x_B \sum_{k=0}^{n} {}^{k}L_{A,B} (x_A - x_B)^k$$

where ${}^{k}L_{A,B}$ is the k-th order interaction parameter which is typically expressed as:

Eq. 2.12: $${}^{k}L_{A,B} = {}^{k}a + {}^{k}bT$$

where ${}^{k}a$ and ${}^{k}b$ are model parameters fit from enthalpy and entropy data. This interaction parameter is very important for modeling.

Stoichiometric compounds have less experimental data available. For a stoichiometric compound, the Gibbs energy can be written as:

Eq. 2.13: $$G^{A_iB_j} = x_A {}^{o}G_A^{SER} + x_B {}^{o}G_B^{SER} + a + bT$$

where $G^{A_iB_j}$ is the molar Gibbs energy of the phase A_iB_j, ${}^{o}G_A^{SER}$ and ${}^{o}G_B^{SER}$ are the molar Gibbs energies of the elements A and B in stable element reference, and a and b are model parameters relating to the enthalpy and entropy respectively.

2.6: Calculation Details

All first-principles calculations were done with the Vienna *Ab-initio* Simulation Package (VASP). The projector augmented wave pseudopotentials were used along with the generalized gradient approximation by Perdew and Wang[11]. The k-point mess was created to obtain approximately 5,000 per reciprocal space atom. A cutoff energy of 300 eV was used. In some instances, multiple relaxation schemes were used to determine which could maintain symmetry.

The CALPHAD evaluation of model parameters was performed in the PARROT module of the Thermo-Calc software. The Cr-Hf-Y system was built from the three individual binaries.

The only compound in the three binary phases, Cr_2Hf, was treated as a stoichiometric compound. There is currently no data for the Cr-Hf-Y system.

2.7: Conclusion

Thermodynamic modeling is dependent on experimental data. Phase equilibria data is more widely available, but it depends on the relationship between two phases. Thermochemical data is preferred because it is associated with a single phase, but this data is much harder to find. In its absence, first-principles calculations can be done to predict this data.

In this thesis, the methods described above are used to model the Cr-Hf-Y system. First-principles are used because of the lack of experimental data. With all the data available, fitting parameters for the various phases are adjusted to best recreate experiments and predict phase stability in the ternary system.

Chapter 3

Thermodynamic Modeling of the Hf-Y System

3.1: Introduction

Experimental data and thermochemical data predicted from first-principles calculations were used to model the Hf-Y system. In this chapter, a review of the available literature will be given, followed by the first-principles calculations, and the current work's thermodynamic modeling.

3.2: Literature Review

The Hf-Y system was investigated by Lundin[12]. In that study, 83 alloys were arc melted. Microscopic examinations of the alloys were determined to be sufficient in inspecting the alloys. Incipient-melting studies were done to determine the solidus temperatures. The low temperature phases, α-Hf and α-Y, are both HCP structure. Both HCP structures transform into BCC at high temperatures as β-Hf and β-Y, and are stable as BCC up to their respective melting points. No compounds are present in the system. A single eutectic point exists, reported at 87.1 at% Y at 1698 K. Small solubilites are listed for both Hf in Y and Y in Hf. The β-Hf $\rightarrow$ α-Hf + Liq eutectoid reaction is speculated from similar systems, but no experimental evidence exists to support it. Liquidus lines are hand drawn with no experimental data to support their shapes. There is no published thermochemical data for the system. Published data is listed in Table 3.1.

3.3: First-Principles Calculations and Radial Distribution Analysis

With the lack of experimental data, first-principles calculations were done on the HCP and BCC solid solutions. Pure element calculations were done and compared to previously published first-principles calculations. The lattice parameters were also compared to experimental data and can be found in Appendix A

Pure Element First-Principles Calculations in Table A.1 and Table A.2. For the mixtures of hafnium and yttrium, both HCP and BCC calculations were done using the special quasirandom structure (SQS) method described in Chapter 2. A 16-atom structure was used for both the BCC[13] and HCP[14] case at compositions of 25, 50, and 75 atomic percent yttrium. Multiple relaxation methods were done for both structures.

For the BCC phase, three relaxation methods were performed with varying degrees of freedom:

1. Volume relaxed method involves changing only the lattice parameters while maintaining the internal angles of the structure. As a result of this, the ratio of the lattice parameters does not change. Relative atom positions are fixed within the cell.
2. Volume and shape relaxed method involves relaxing the lattice parameters as well as the changing the shape of the cell. This method will change the internal angles of the structure and change the ratio of the lattice parameters. Relative atom positions are fixed within the cell.
3. Fully relaxed method involves the changing the lattice parameters, the internal angles, and the relative atom positions. This method will relax the ratio of the lattice parameters as well as the previous method.

The symmetry of each relaxed structure was investigated by looking at their radial distribution (RD). Figure 3-1 shows the RD results for the BCC Hf-Y SQS at 50 at% Y. This RD analysis is representative of all three compositions studied. The ideal structure is compared to the three relaxations. The fully relaxed case shows great deviation from the ideal structure as atoms are not clustered around their original lattice sites. The volume relaxed and the volume and shape relaxed methods both appear to have maintained the symmetry. As stated in Chapter 2, the relaxation method chosen should have the initial structure in mind. Since a BCC structure only has one degree of freedom, the volume relaxed method was determined to best represent the phase.

The HCP case is a more complex than the BCC case. Unlike BCC, which has only one independent lattice parameter, the HCP structure is defined by two lattice parameters, more specifically the *a* lattice parameter and the *c/a* lattice parameter ratio. The relaxation methods were the same as described before, but there was one difference. Since the volume relaxed method keeps all of the internal angles fixed, this means the *c/a* ration is not relaxed. To overcome this, a matrix approach was taken. The *a* and *c/a* ratio were manually adjusted and static calculations were performed at each change to create an energy surface plot. The minimum of the plot was determined and a final calculation was done to verify it would indeed by the minimum.

Figure 3-2 shows the RD results for the HCP Hf-Y SQS at 50 at % Y. This analysis is representative of the three compositions studied. The ideal structure is compared to the three relaxation methods. Again, the fully relaxed method deviates from the ideal structure. For the volume relaxed case, which involves the static-matrix calculations, the "relaxed" structure is exactly the same as the ideal structure since it was a static calculation. The RD analysis of the volume and shape relaxed method shows the symmetry was preserved. Another good indication was that the static-matrix calculation resulted in the same total energy as the volume and shape

relaxed method. The volume and shape relaxed method was used because of the computational time saved by running one calculation versus running many static calculations.

According to Eq. 2.4, the enthalpies of mixing can be determined from the first-principles calculations. The large positive enthalpy of mixing values correspond to the fact that there is very limited solubility in both phases. These values were used to model the solid phases.

3.4: Thermodynamic Modeling

The pure element database was used in this modeling. The enthalpy of mixing data from first-principles calculations allows for a more unique description of the Gibbs energy functions of the BCC and HCP phases. These phases were both treated as regular solutions. Figure 3-3 and Figure 3-4 show the enthalpy of mixing for the BCC and HCP phases, respectively, which were derived from first-principles calculations. The liquid phase was then modeled as a subsubregular solution with the limited phase equilibria data. The interaction parameters are listed in Table 3.2. The phase diagram, shown in Figure 3-5, has an advantage over the previous hand-drawn phase diagrams.

Lundin and Klodt[12] speculated that there should be a eutectoid reaction in the hafnium-rich BCC to HCP transition. Based on the enthalpy of mixing data for the two phases, it was shown that HCP was more stable than BCC, leading to a peritectic reaction instead. This is a much more meaningful diagram, as the eutectoid reaction was based only on the fact that other systems show similar behavior, rather than on data.

3.5: Conclusion

Modeling the Hf-Y binary system is the first step to completing the Cr-Hf-Y system. First-principles calculations were done on the BCC and HCP phases. Attention was paid to the degrees of freedom of each structure as well as the symmetry after relaxation. By using the data from the first-principles calculations, the enthalpy of mixing for the two phases was modeled. Adding this modeling to the phase equilibria data, the Hf-Y system was model. While previous investigations had assumed a eutectoid reaction existed in the hafnium rich region, this work found a peritectic reaction instead.

Table 3.1: Invariant Equilibria for Hf-Y System

Reaction	Type	T (K)	Liquid at. %Y	Reference
Liquid ⟷ α-Hf + αY	Eutectic	1684	89.3	This Work
		1698	87.1	[12]

Table 3.2: Interaction parameters in the Hf-Y system

Phase	Interaction Parameters
BCC	${}^{0}L^{BCC} = 79517$
HCP	${}^{0}L^{HCP} = 64776$
Liquid	${}^{0}L^{Liquid} = 4782 + 12.162T$
	${}^{1}L^{Liquid} = -1975$
	${}^{2}L^{Liquid} = 5756$

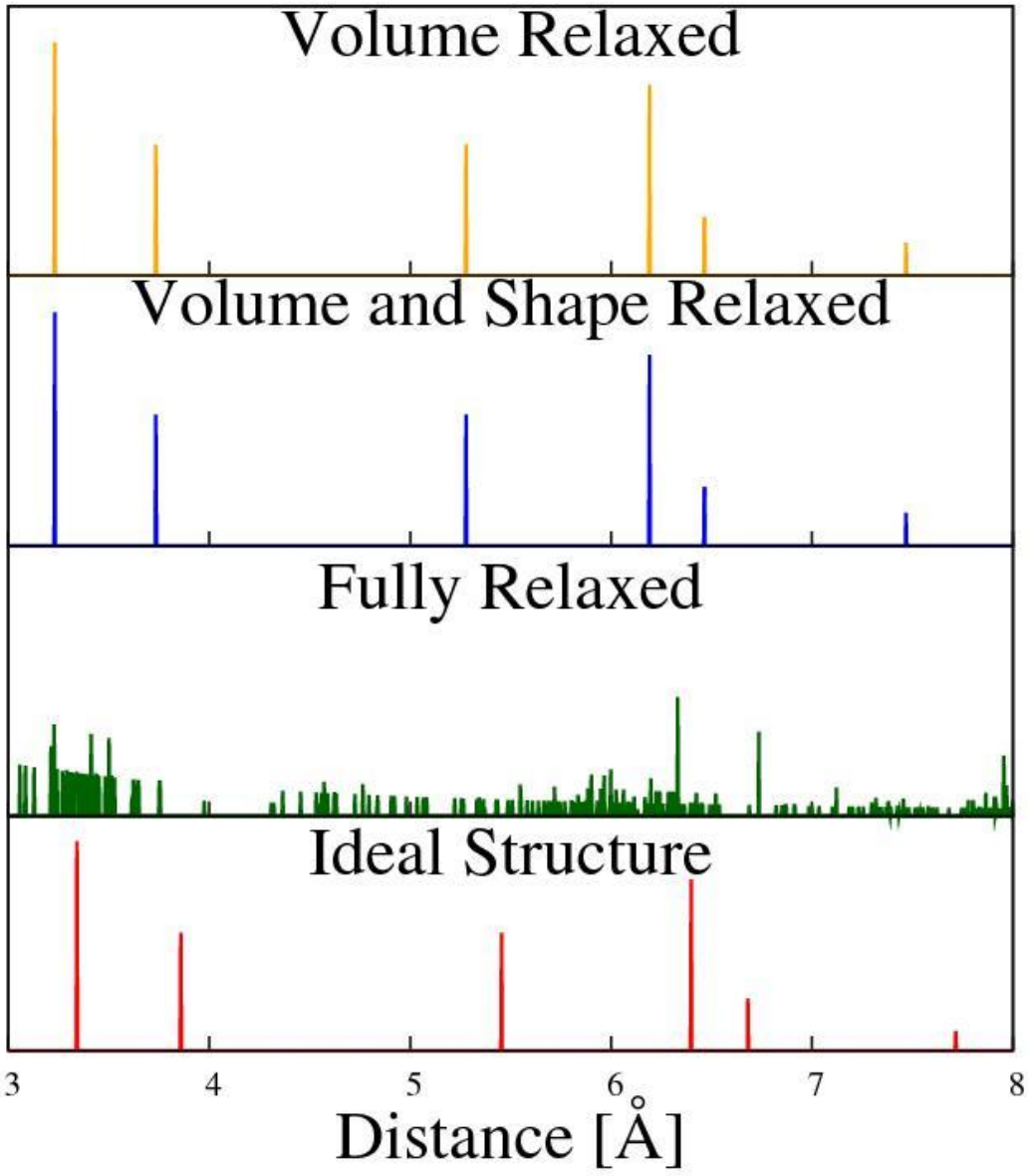

Figure 3-1: The radial analysis of a 50:50 Hf-Y BCC SQS calculation showing a loss of symmetry in the fully relaxed case and symmetry preserved in the volume relaxed case.

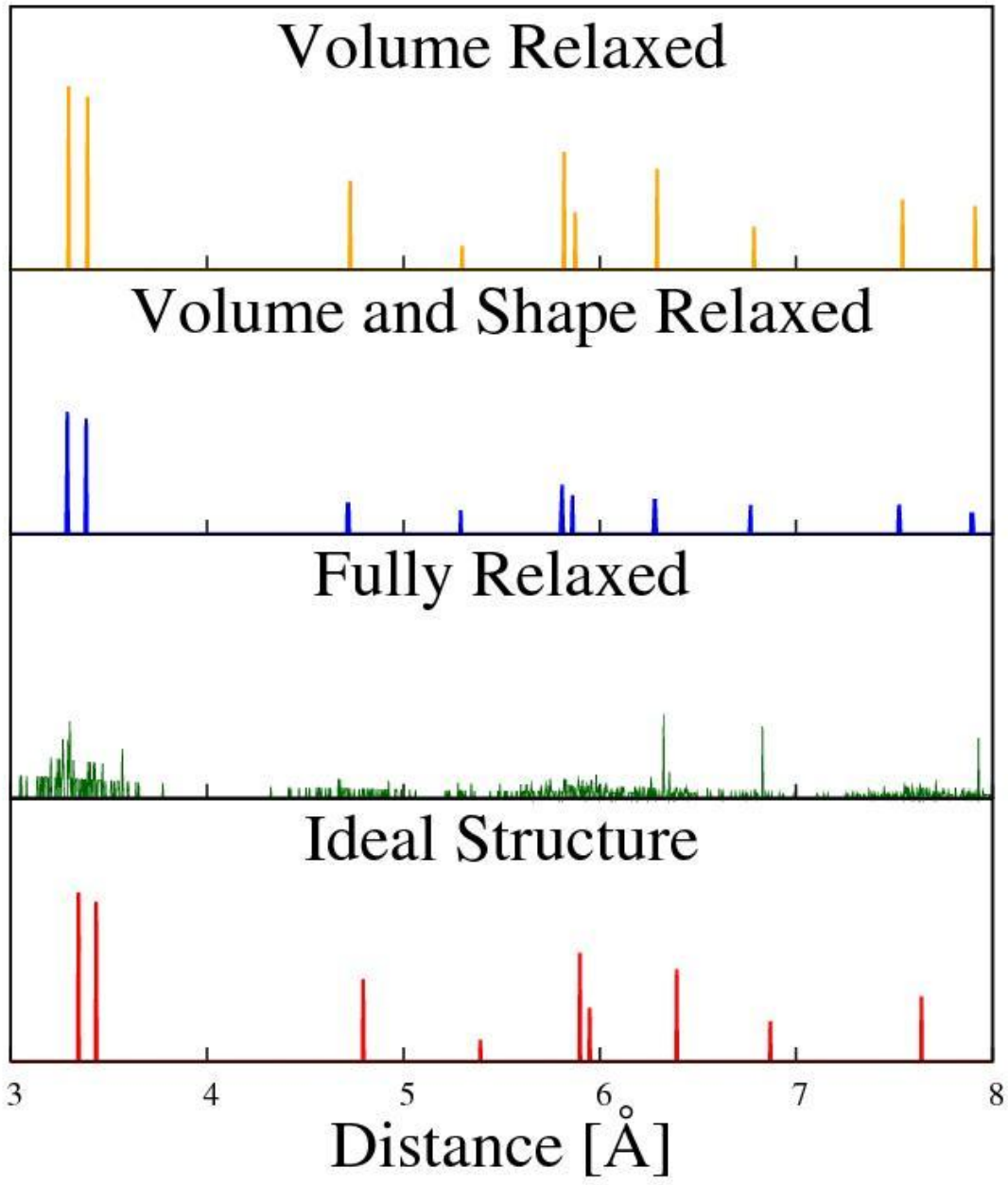

Figure 3-2: The radial analysis of a 50:50 Hf-Y HCP SQS calculation showing a loss of symmetry in the fully relaxed case and symmetry preserved in the volume and shape relaxed case.

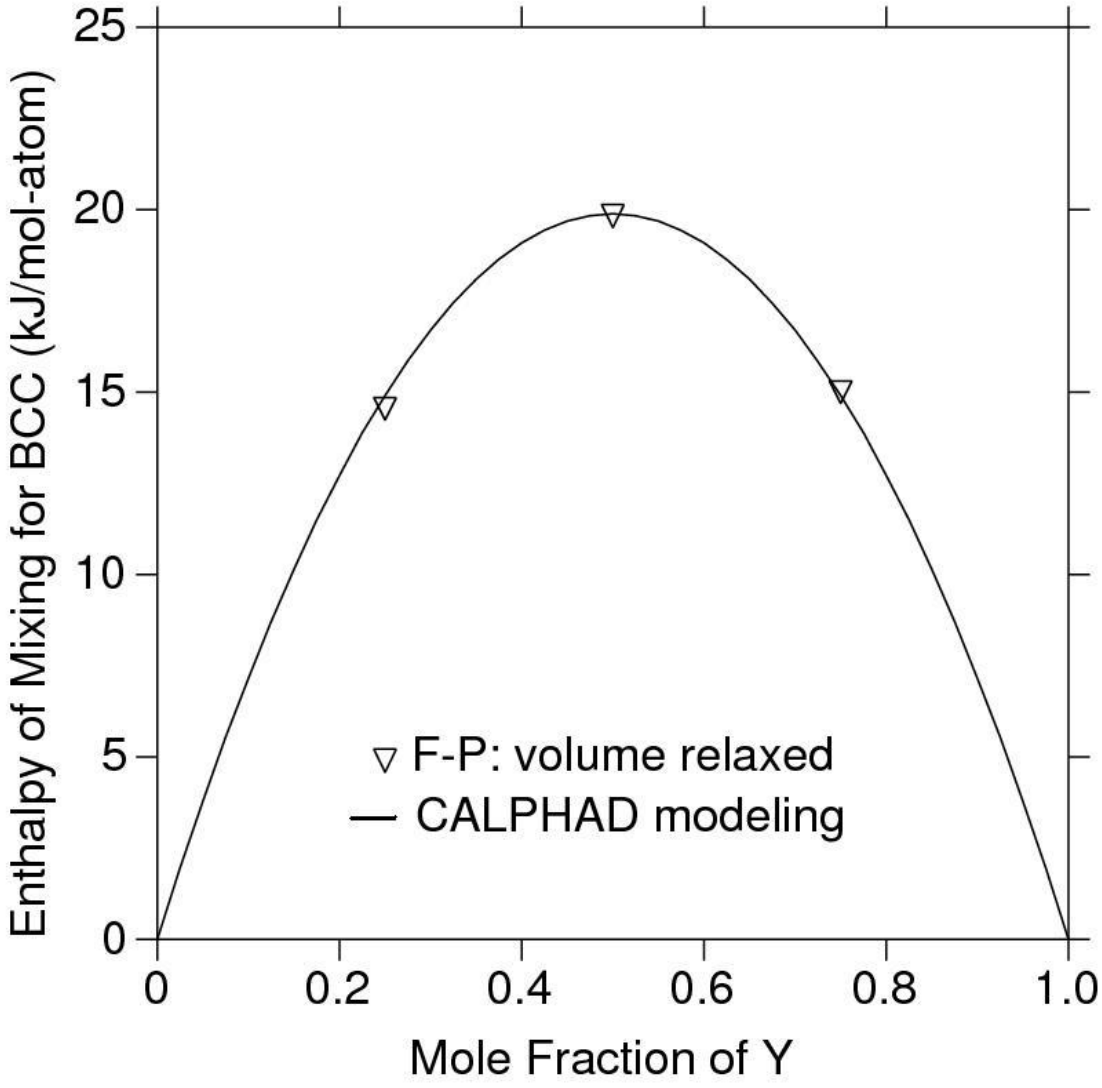

Figure 3-3: The enthalpy of mixing for the BCC phase showing the data obtained from the volume relaxed first-principles calculations and the modeling of that data in ThermoCalc.

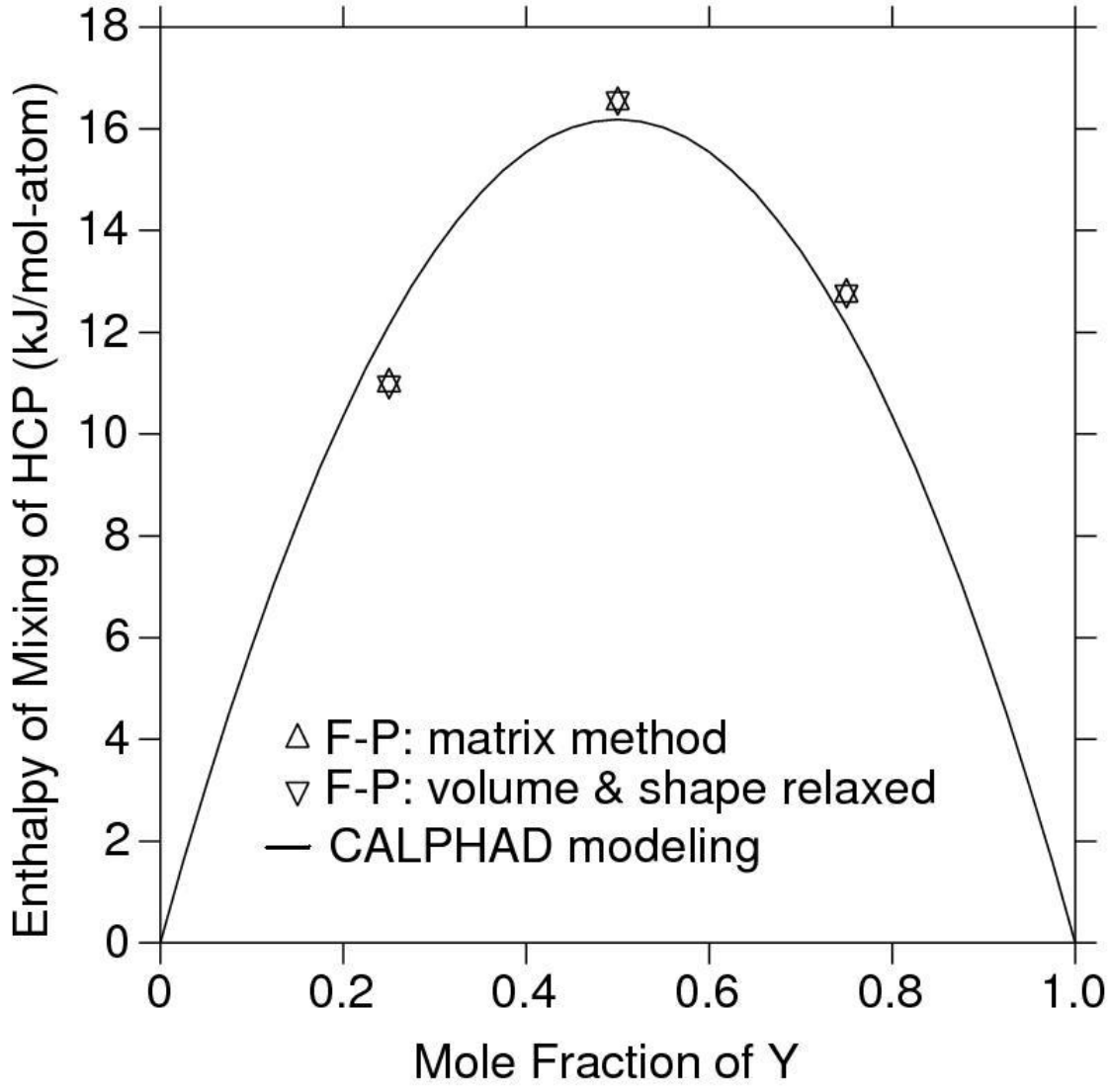

Figure 3-4: The enthalpy of mixing for the HCP phase showing the data obtained from first-principles calculations, both the static matrix approach and the volume and shaped relaxed method, and the modeling of that data in ThermoCalc.

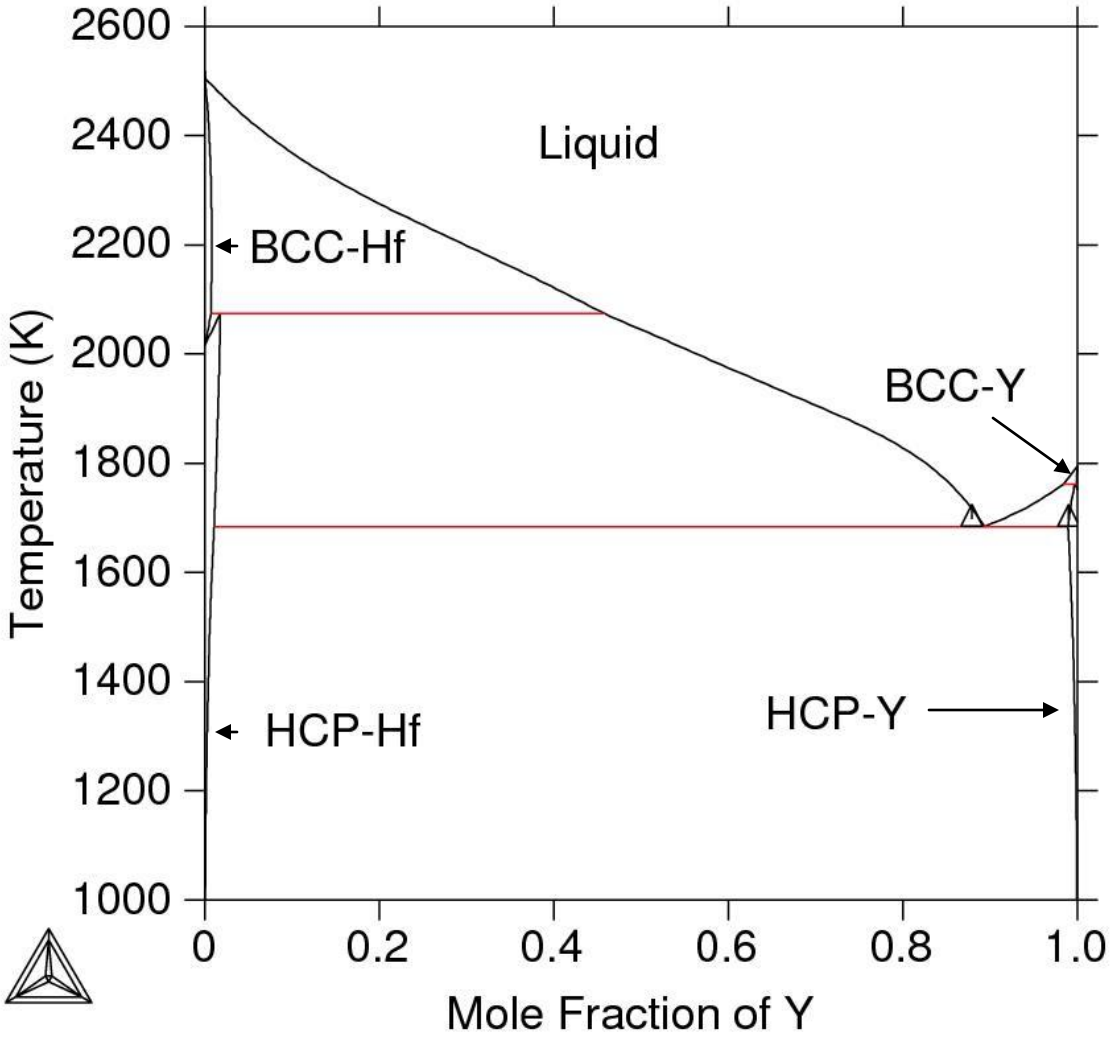

Figure 3-5: Calculated Hf-Y phase diagram with phase equilibria data from Lundin and Klodt[12]

Chapter 4

Thermodynamic Modeling of the Cr-Y System

4.1: Introduction

Experimental data and thermochemical data predicted from first-principles calculations were used to model the Cr-Y system. In this chapter, a review of the available literature will be given, followed by the first-principles calculations, which involve antiferromagnetic BCC Cr and ferromagnetic HCP Cr, and the current work's thermodynamic modeling.

4.2: Literature Review

An initial experimental investigation into the Cr-Y system was done by Terekhova[15]. Microscopic examinations were used to determine solubility. The drop method was used to determine the solidus temperatures. In this method, a hole was drilled into the sample, which was heated by passing current through it. The temperature was recorded just prior to a drop of liquid metal forming. A liquid miscibility gap was reported as well as extremely limited solubility.

Venkatraman and Neumann[16] suggested two different phase diagrams: one without a miscibility gap and one with a large miscibility gap. Their work cites unpublished and technical reports which are difficult to obtain. Okamoto reviewed the Cr-Y system[17] and stated the phase diagram without the miscibility gap is thermodynamically improbable based on trends described in previous work[18]. Okamoto's diagram supports a miscibility gap in the liquid region, but has a eutectic point at a more yttrium-rich composition. Chan modeled the Cr-Y

system[19] and also found a eutectic point in agreement with Okamoto, although Chan did not use any first-principles calculations for modeling. Phase equilibria data is available in Table 4.1

It is known that the ground state of BCC chromium is antiferromagnetic (AFM) and has been shown computationally that the ground state for HCP chromium is a very weak ferromagnetic (FM) one[20]. Moruzzi and Marcus[21] suggest that to calculate the AFM state for BCC chromium, a four-atom supercell should be used.

4.3: First-Principles Calculation and Radial Distribution Analysis

First-principles calculations were done on the BCC and HCP phases. Pure element calculations were done and compared to previously published first-principles calculations and experimental data. A summary of the pure element calculations can be found in Appendix A

Pure Element First-Principles Calculations in Table A.2 and Table A.3. The same 16-atom supercell that was used for the Hf-Y system was used for BCC[13] and HCP[14] phases, as well as the same relaxation methods. Briefly, a relaxation of the volume by changing the lattice parameters, a relaxation of the volume and shape by changing the lattice parameters and the internal angles of the structure, and a full relaxation of the lattice parameters, internal angles and atom positions were done. A 25, 50 and 75 atomic percent yttrium calculation was done. Figure 4-1 shows the RD analysis for the BCC SQS structure. This shows the RD analysis for the 50 at% Y composition and is representative of all the other BCC SQS calculations done. We see the same result as in the Hf-Y system. There is a loss of symmetry with the fully relaxed calculation, whereas the volume relaxed calculation maintains symmetry and has the same number of degrees of freedom as the initial structure. The volume relaxed calculation was used as it best represented the solid solution. For the HCP SQS calculations, the static-matrix approach was only done one

time once the volume and shape relaxed calculations were shown to maintain symmetry, as seen in Figure 4-2.

For the BCC calculations of pure chromium, a one-atom FM calculation and a one-atom nonmagnetic (NM) calculation was done as well as a four-atom AFM calculation. The AFM calculation was found to have the lowest energy per atom. Simply by looking at the 4-atom supercell for pure chromium, it became apparent which two atoms should have the same spin to give the AFM configuration. In the SQS 16-atom supercell, it is not so obvious. To overcome this, multiple configurations of positive and negative magnetic moments were used on various atoms. It was found that the nonmagnetic calculations resulted in a higher total energy than the total energy of the magnetic calculations, indicating that the magnetic states were more stable. All of the magnetic calculations resulted in very similar energies, much different than the nonmagnetic values in most cases. Figure 4-3 shows formation energies of different magnetic configurations. While it isn't possible to know which magnetic configuration is correct, the energies were all close enough that an average was taken. This provided a good value to use as the enthalpy of mixing for the BCC phase. The HCP phase was found to have a lower energy FM structure than the NM structure.

4.4: Thermodynamic Modeling

The pure element database was used in this modeling. The enthalpy of mixing data was determined from the first-principles calculations. This data allows for a more unique Gibbs energy description of the phases. Figure 4-4 and Figure 4-5 show the enthalpy of mixing data for the BCC and HCP phases, respectively. Both phases were treated as subregular solution phases. The large enthalpy of mixing values for solid phases are indicative of the extremely limited solubility limits. The liquid miscibility gap was modeled as well. The only data points for the

miscibility gap were the end points at 2033 K. The interaction parameters of all three phases are listed in Table 4.2.

While the experimental data from Terekhova[15] was used to model the system, this modeling work found similar results to Chan[19]. The Y-rich eutectic point was experimentally shown to be at a lower Y concentration than both Chan's work as well as this work. However, this work was better able to model the temperature of that reaction. This work also was able to model the monotectic reaction, both in terms of composition and temperature. A comparison of these two models can be found in Table 4.1.

4.5: Conclusion

After modeling the Hf-Y system, the next system that was modeled was the Cr-Y system. First-principles calculations were done on the BCC and HCP phases. In addition to paying attention to the symmetry of the phases, multiple magnetic configurations were used to help determine the enthalpy of mixing values for the BCC phase. The HCP phase was determined to be ferromagnetic, as it has been reported in literature. Using the enthalpy of mixing values from first-principles, the Cr-Y system was modeled. This modeling work more accurately represents the experimental data than previous modeling attempts.

Table 4.1: Invariant Equilibria for Cr-Y System

Reaction	Type	T (K)	at %Y		Reference
$Liquid_1 \leftrightarrow Liquid_2 + Cr$	Monotectic	2034	14.5	58.2	This Work
		2033 ± 25	9.36	57.71	Exp. [15]
		2033 ± 25	9	58	[16]
		2013	10.9	61.1	[17]
		2020	18.5	55.2	CALPHAD[19]
Liquid ↔ Cr + αY	Eutectic	1589	87.2		This Work
		1588 ± 7	79.7		Exp. [15]
		1603 ± 25	80		[16]
		1573	85.9		[17]
		1602	87.1		CALPHAD[19]

Table 4.2: Interaction parameters in the Cr-Y system

Phase	Interaction Parameters
BCC	${}^0L^{BCC} = 300000$
	${}^1L^{BCC} = 230000$
HCP	${}^0L^{HCP} = 260000$
	${}^1L^{HCP} = 150000$
Liquid	${}^0L^{Liquid} = 32481$
	${}^1L^{Liquid} = 10066$

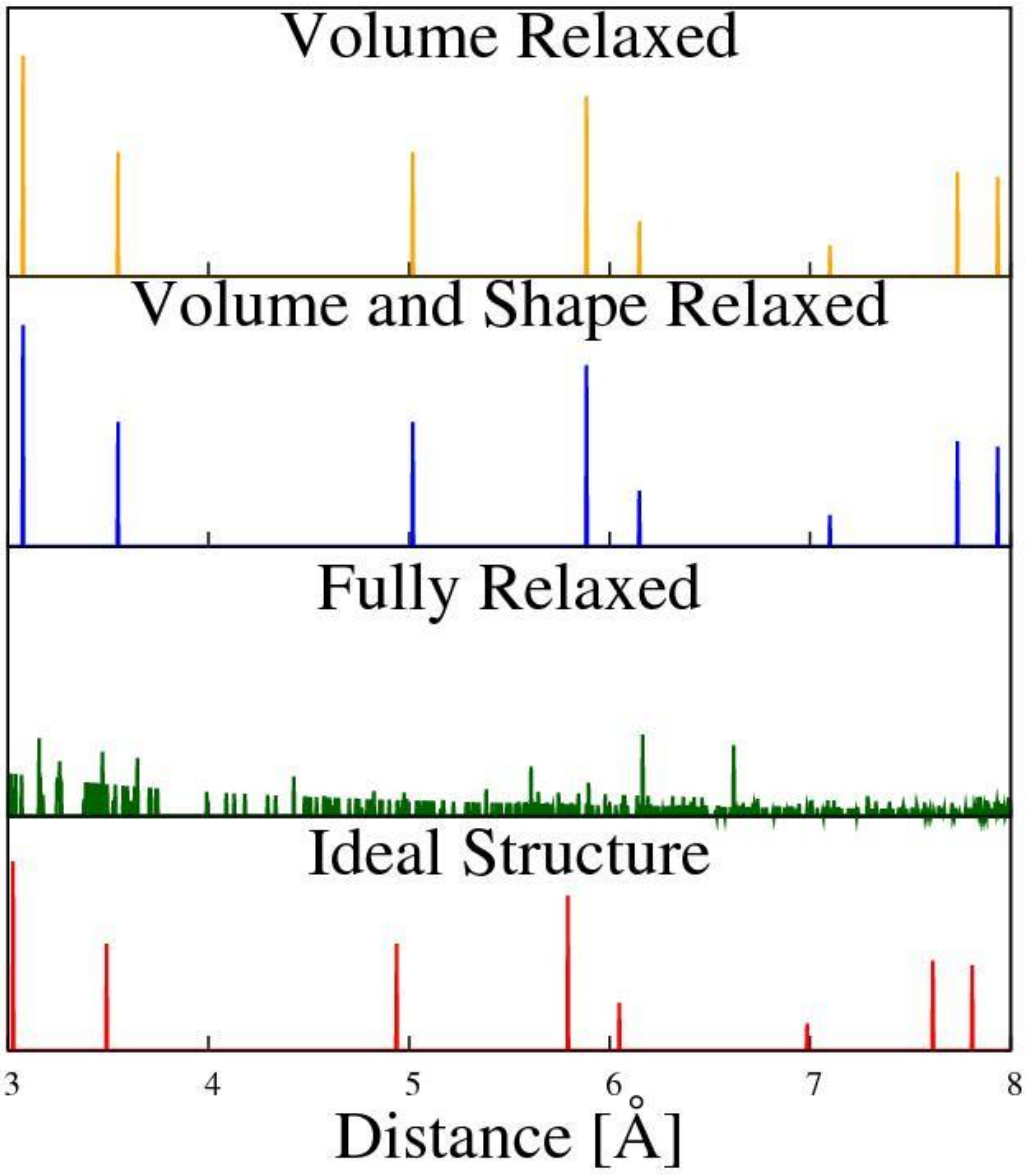

Figure 4-1: The radial analysis of a 50:50 Cr-Y BCC SQS calculation showing a loss of symmetry in the fully relaxed case and symmetry preserved in the volume relaxed case.

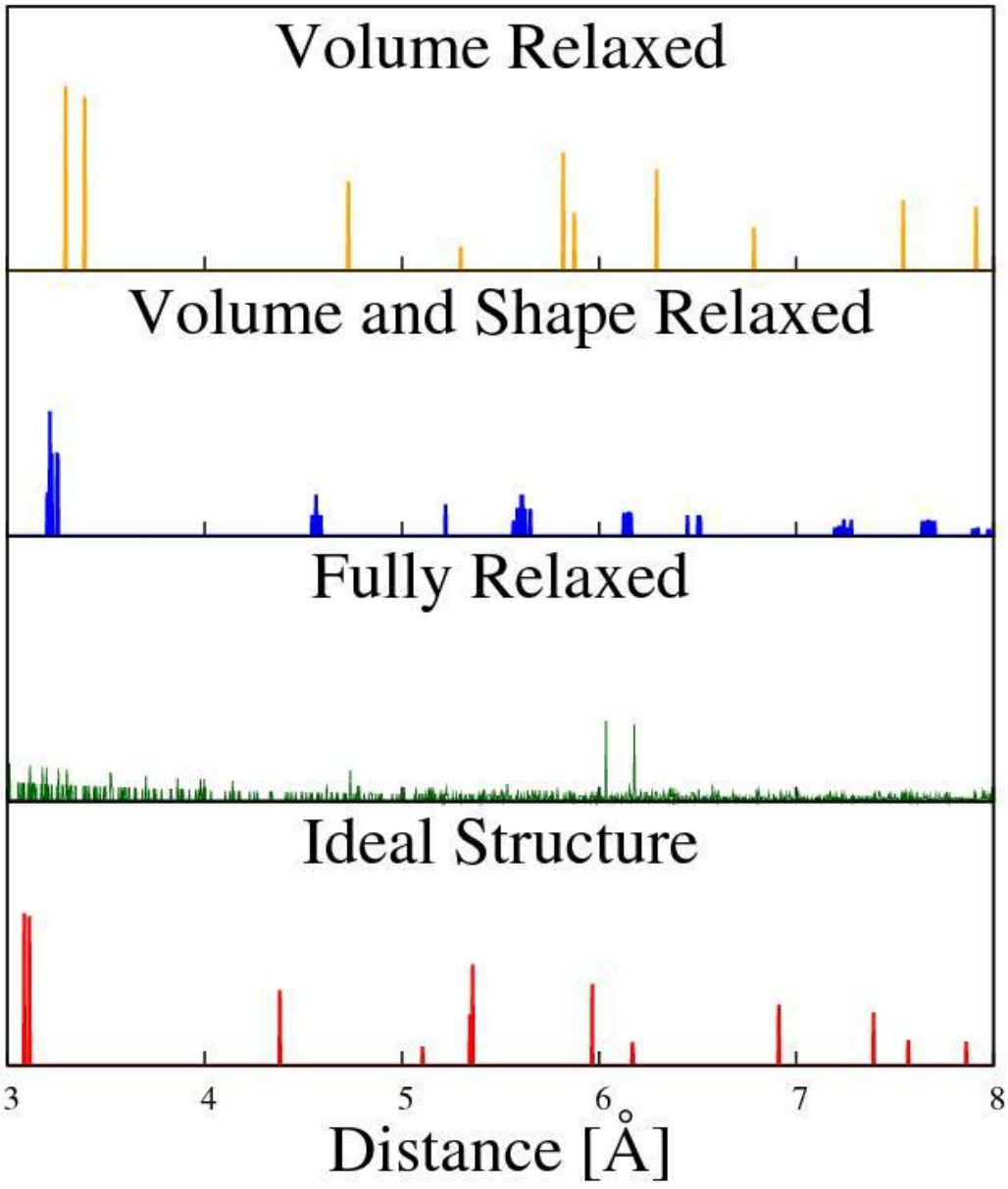

Figure 4-2: The radial analysis of a 50:50 Cr-Y HCP SQS calculation showing a loss of symmetry in the fully relaxed case and symmetry preserved in the volume and shape relaxed case.

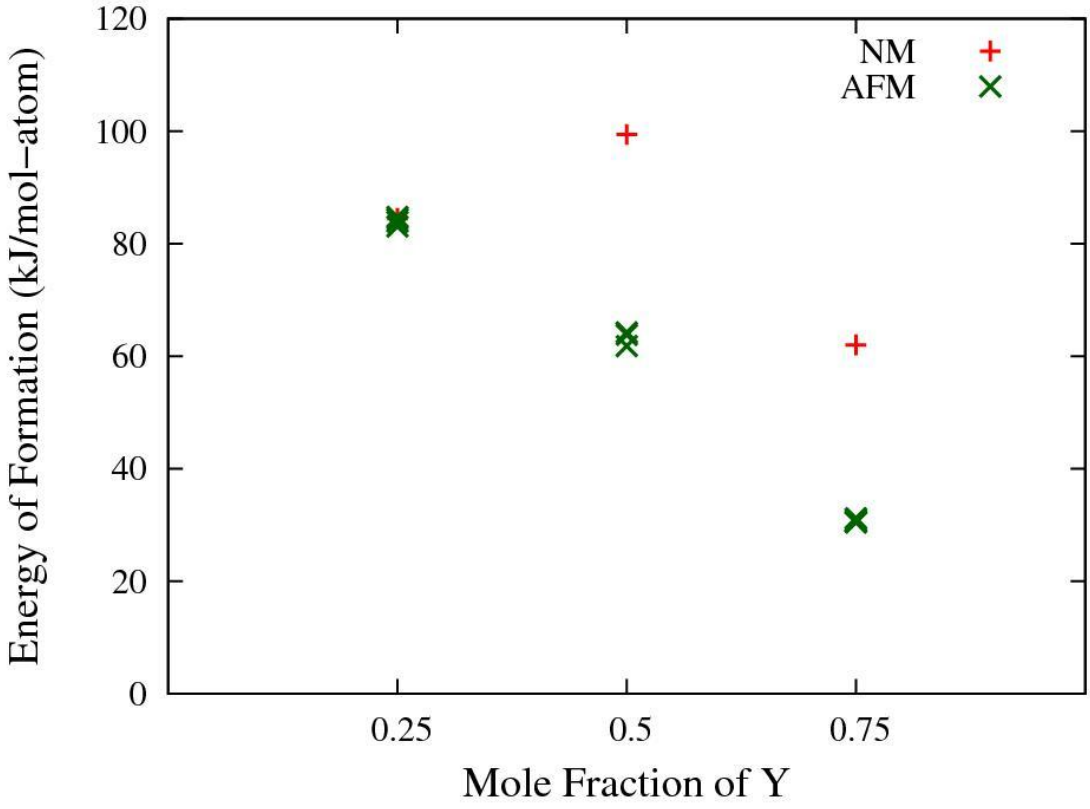

Figure 4-3: The energy of formation values for BCC SQS calculations of nonmagnetic (NM) and antiferromagnetic (AFM) configurations. Various configurations were tested since the true magnetic structure was unknown. Since all AFM values were similar to the other configurations, and much different than the NM structures in most cases, an average of the AFM configurations was used for modeling.

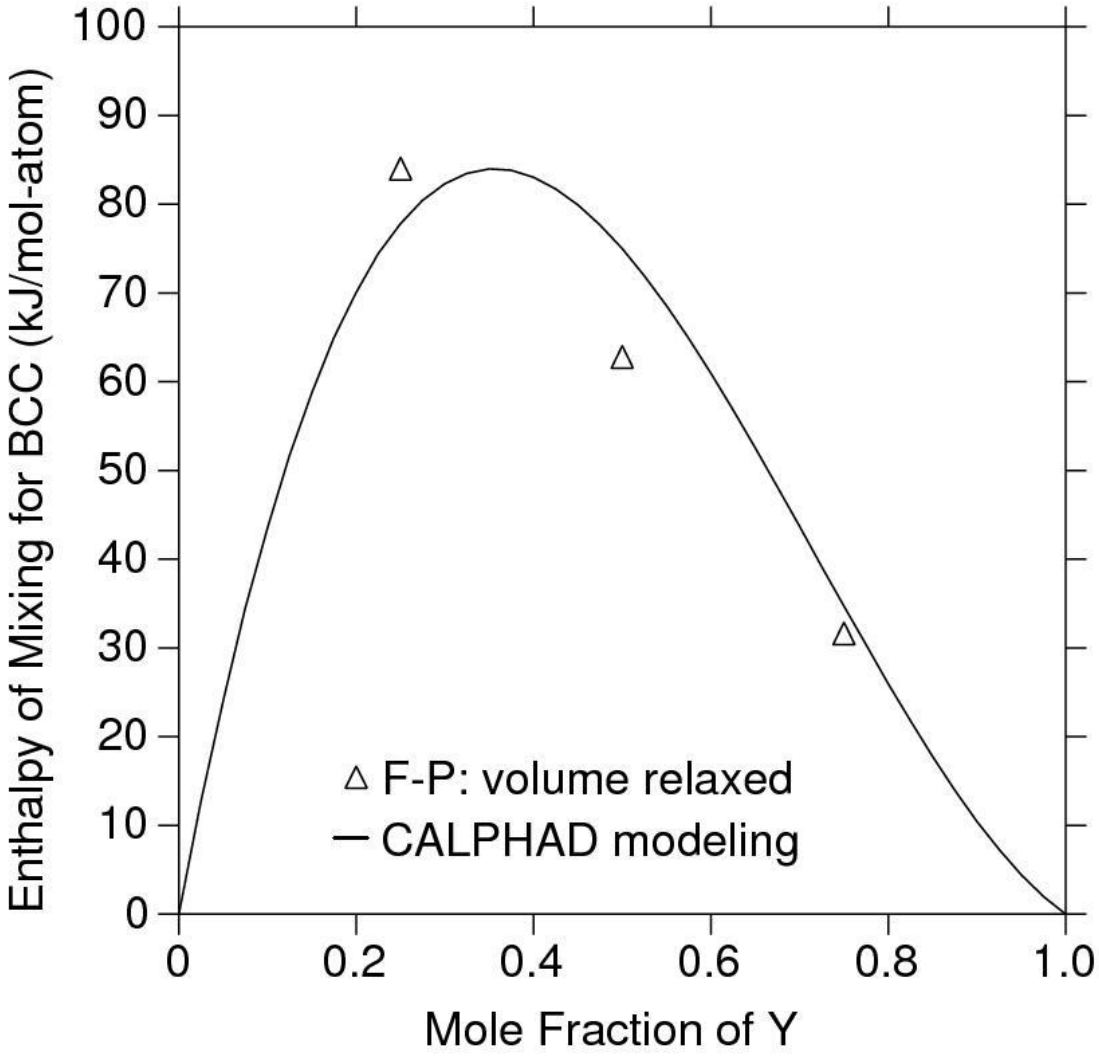

Figure 4-4: The enthalpy of mixing for the BCC phase showing the data obtained from the magnetic volume relaxed first-principles calculations and the modeling of that data in ThermoCalc.

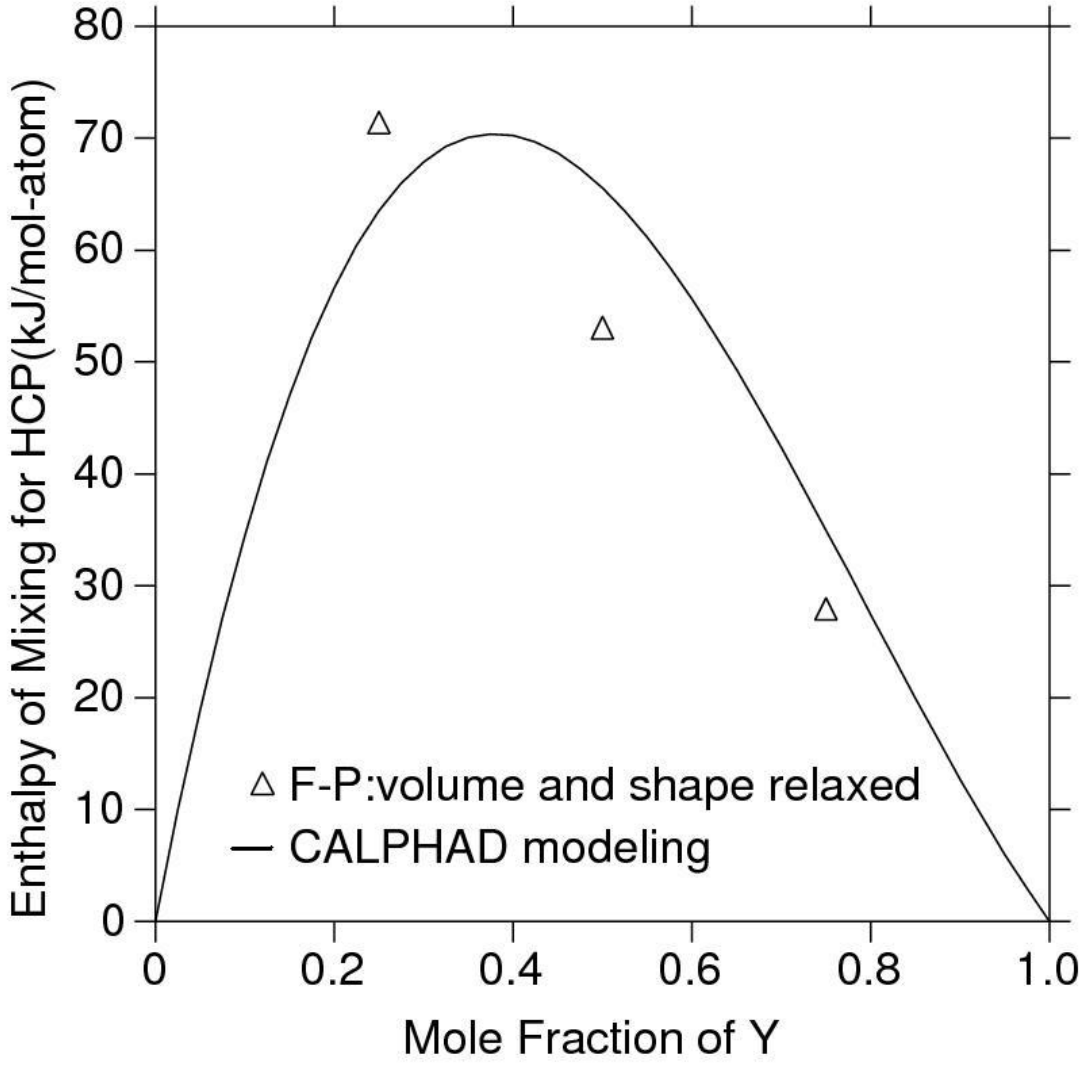

Figure 4-5: The enthalpy of mixing for the HCP phase showing the data obtained from the magnetic first-principles calculations and the modeling of that data in ThermoCalc.

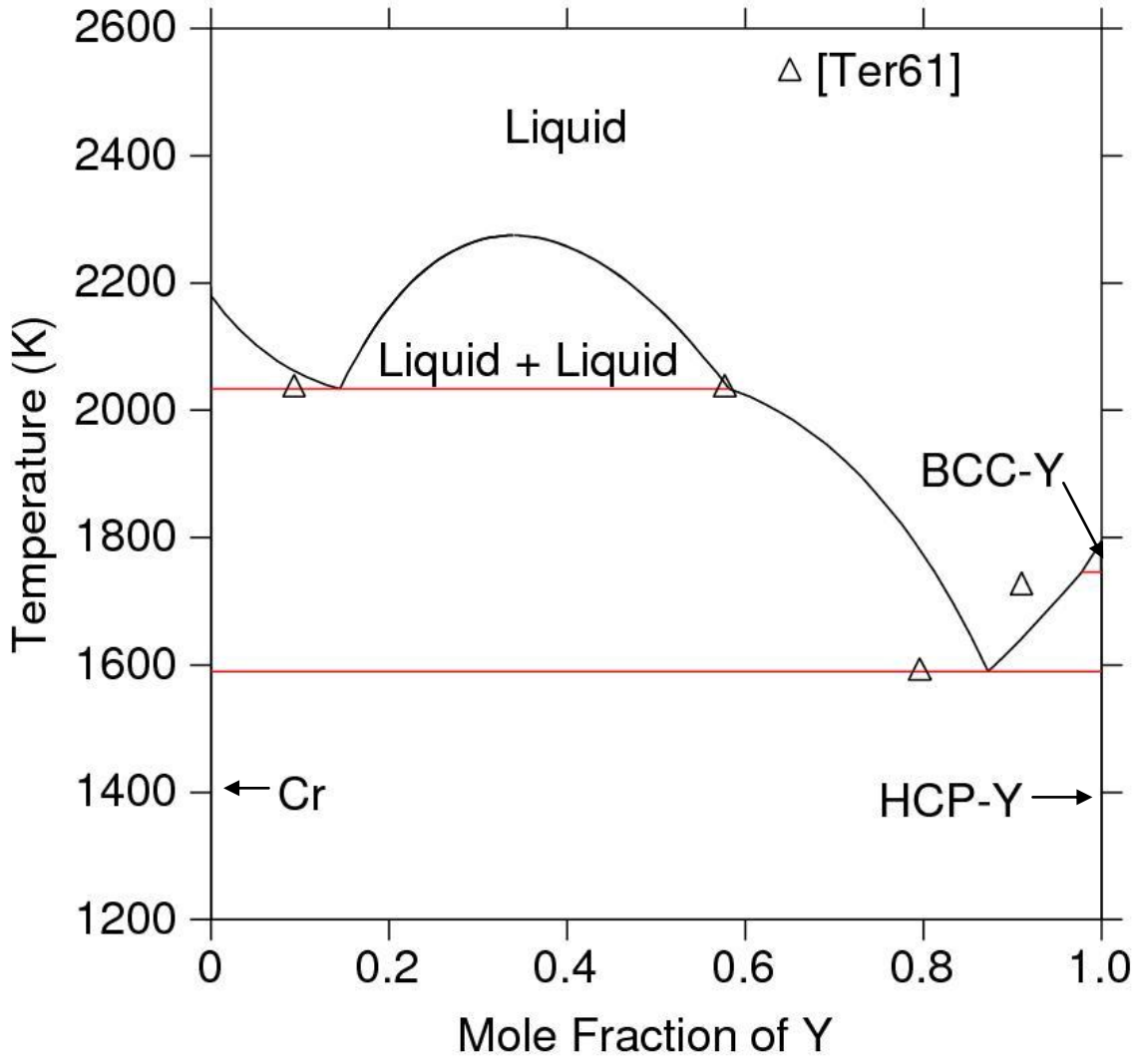

Figure 4-6: Calculated Cr-Y phase diagram with phase equilibria data from Terekhova[15]

Chapter 5

Thermodynamic Modeling of the Cr-Hf System

5.1: Introduction

In this chapter, experimental data was used to model the Cr-Hf binary system. There is some disagreement between sources as to which phases are present. This chapter will review the available literature and discuss why it is unclear which phases exist in the phase diagram, followed by the modeling of the Cr-Hf system.

5.2: Literature Review

The Cr-Hf system has been reviewed by Yang et al.[22]. Experimental studies of the system were done by Carlson and Alexander[23], Svenchinkov et al.[24] and Rudy and Stefan[25]. Each of these studies showed similar results with respect to the phase diagram. Chromium was always BCC as a solid, hafnium was HCP at low temperatures and BCC at high temperatures, and there was one Laves phase compound, Cr_2Hf. Rudy and Stefan[25] found only one form of the Laves phase, the hexagonal C14 form. Carlson and Alexander found the Laves phase was dimorphic, with a cubic C15 phase stable at low temperatures and the C14 phase at high temperatures. Differences in the temperatures and compositions of the invariant reactions, as well as solubility ranges of the compound were present between the three studies, but the general features of the phase diagram were consistent.

Venkatraman and Neumann[26] also reviewed the system and noted the low temperature form of the Laves phase was the cubic C15 phase and the high temperature form was the

hexagonal C14 phase. It was also noted that a third modification of the Laves phase had been reported but not corroborated by another investigation. But a second study has been done that was not reported by Venkatraman and Neumann. Minayeva et al.[27] reported finding the C36 form of the Laves phase between the low temperature and high temperature polymorphs. By annealing samples between 1300 and 1600^{o}F for 1300 hours[28], the C36 Laves phase was detected. It has been said that the transitions between Laves phases are very sluggish[23, 25]. This may be the reason it was so difficult to determine which phases were present.

First-principles calculations were done on the three polymorphs of the Laves phase by Chen et al.[29]. The enthalpy of formation for each structure was calculated using antiferromagnetic BCC chromium and nonmagnetic HCP hafnium. These values were used in modeling the stability of the Laves phases.

5.3: Thermodynamic Modeling

The first-principles calculations from Chen et al.[29] were used to help model the Laves phases. The enthalpy of formation values were used as the *a* term in Eq. 2.12. By adjusting the *b* term from the same equation, a Gibbs energy diagram was created to recreate the transition temperatures given by Minayeva[27]. The Gibbs energy of the Laves phases can be seen in Figure 5-1. Note the pure element database is used for this modeling. It should also be noted that the Laves phase was modeled as a stoichiometric compound for simplicity. The remaining phases were modeled with the experimental data from Carlson and Alexander[23], Svenchinkov et al.[24] and Rudy and Stefan[25].

This modeling work is in better agreement with the experimental data than the work done by Yang et al.[22]. A summary of the invariant reactions can be found in Table 5.1 and the phase

diagram can be found as Figure 5-2. Also included are the phase descriptions and interaction parameters in Table 5.2.

5.4: Conclusion

With first-principles calculations already performed on the Cr_2Hf Laves phase, this system was modeled with enthalpy of formation values of the Laves phase and experimental phase equilibria data. This modeling work improves on previous work for Yang et al.[22] by including all three polymorphs of the Laves phase and more accurately representing the experimental data into the model

.

Table 5.1: Invariant Equilibria for Cr-Hf System

Reaction	Type	T (K)	at %Cr			Reference
Liquid ↔ BCC(Cr) +	Eutectic	1952	86.9	66.67	99.8	This Work
Cr_2Hf		1915±10	88	68	100	Exp[24]
		1935±15	86	66.5	100	Exp[23]
		1966±15	87±2	67	>98	Exp[25]
		1938±30	87	67	100	[26]
		1954	85.7	69	98.2	CALPHAD[22]
Liquid ↔ BCC(Hf) +	Eutectic	1724	33.04	9.5	66.67	This Work
Cr_2Hf		1665±10	27		64	Exp[24]
		1765±5	31	16	64.5	Exp[23]
		1785±8	41±2	13±1	64	Exp[25]
		1773±20	30	16	65	[26]
		1787	36	15.3	65	CALPHAD[22]
BCC(Hf) ↔ Cr_2Hf +	Eutectoid	1636	8.98	0.1	66.67	This Work
HCP(Hf)		1575±10	8.5	<2	66	Exp[24]
		1665	12	<1.2	66.5	Exp[23]
		1630±15	11.5±1	<2	65	Exp[25]
		1643±20	12	<2	65	[26]
		1624	11.5	2	65	CALPHAD[22]

Table 5.2: Phase description for the Cr-Hf system. The values of G^{Cr} and G^{Hf} can be found in Appendix C.

Phase	Interaction Parameters
Cr_2Hf C15	${}^0G^{C15} = 2G^{Cr} + G^{Hf} - 34900 - 2.07T$
Cr_2Hf C36	${}^0G^{C36} = 2G^{Cr} + G^{Hf} - 32500 - 3.70T$
Cr_2Hf C14	${}^0G^{C14} = 2G^{Cr} + G^{Hf} - 29600 - 5.50T$
BCC	${}^0L^{BCC} = 20000 + 6.00T$
	${}^1L^{BCC} = 30000 - 5.50T$
HCP	${}^0L^{HCP} = 30000$
	${}^1L^{HCP} = -10000$
Liquid	${}^0L^{Liquid} = -20000$
	${}^1L^{Liquid} = 6000$

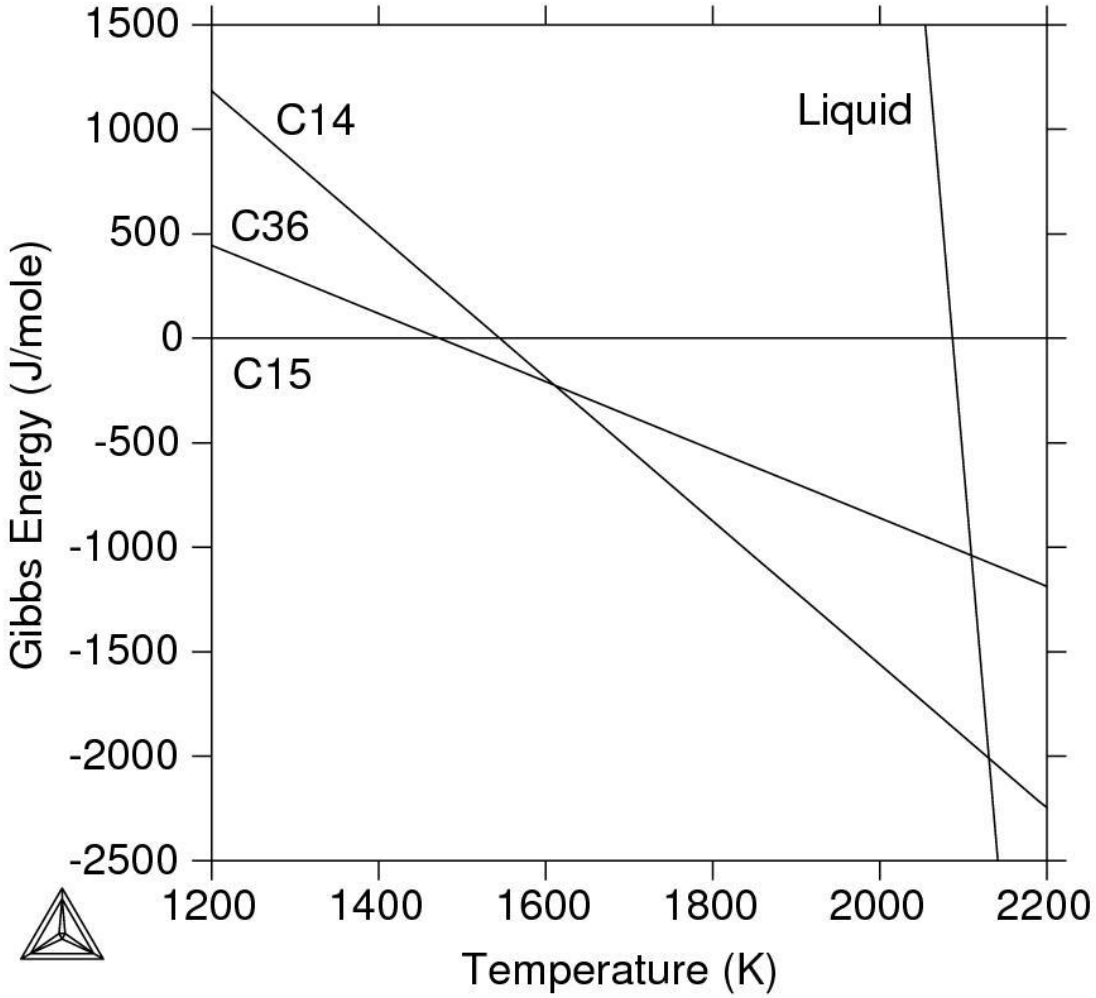

Figure 5-1: The Gibbs energy for the different polymorphs of the Laves phase. By adjusting the interaction parameters, the transition temperatures were recreated based on experimental data.

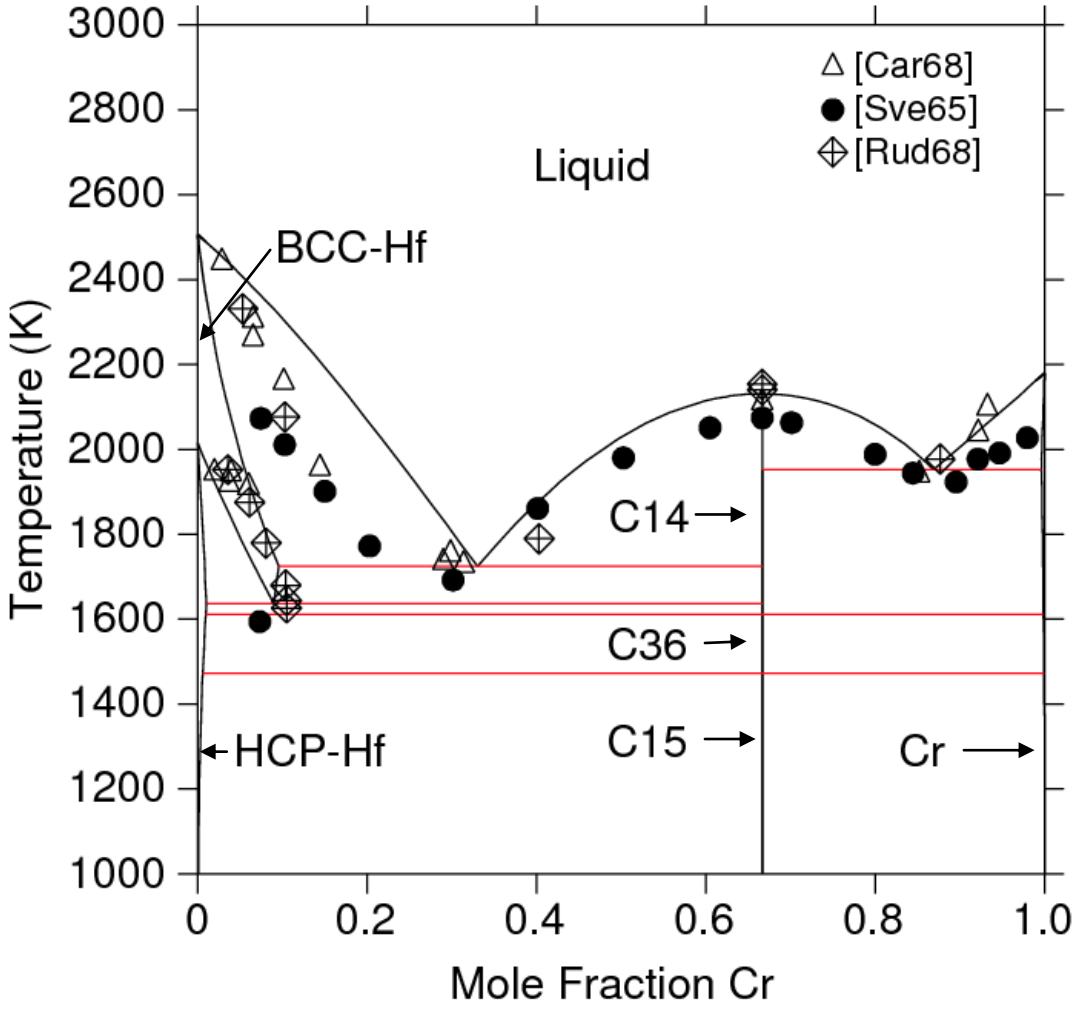

Figure 5-2: Calculated Cr-Hf phase diagram with phase equilibria data from Carlson and Alexander[23], Svenchinkov et al.[24] and Rudy and Stefan[25].

Chapter 6

Thermodynamic Modeling of the Cr-Hf-Y System

6.1: Introduction

With all three constituent binary phase diagrams modeled, the Cr-Hf-Y ternary system can now be modeled. There is no published data for this system. This chapter will discuss the combination of the three binary phase diagrams into the ternary system.

6.2: Literature Review

The ternary phase diagram can be extrapolated from the binary systems. Experimental data of the ternary system is typically added to the model. However, no literature was found for this ternary system. There are also no known ternary compounds.

6.3: Thermodynamic Modeling

With no experimental data available and no ternary compounds, the modeling of this system involved the combination of the binary systems. The modeling uses the pure element database as did the three binary systems. All parameters remained unchanged. Isothermal sections are available in Appendix B.

By looking at the isothermal sections, the presence of the Laves phase can be detected at different temperatures. It is known that this phase will be detrimental to the nickel superalloy and should be avoided. Without nickel included in this system, it becomes very

difficult to show how this ternary system will be used for the overall processing of the alloy. However, the usefulness of these types of diagrams can be seen. Examining phase stability can create great processing advantages.

One prediction that can be seen is the existence of a ternary liquid miscibility gap. At 2200 K, the liquid miscibility gap exists in the Cr-Y binary system. However, when the system is cooled to 2000 K, the miscibility gap is no longer stable in the binary, but has extended and become stable in the ternary system. Even at 1800 K, the miscibility gap is still present.

6.4: Conclusion

The three binary systems were combined to form the Cr-Hf-Y ternary system. Isothermal sections and a liquidus project were modeled. By examining the phase stability of the ternary phase, unwanted phases can be avoided during processing. This will give a scientific processing advantage over a trial and error processing method.

Chapter 7

Conclusions and Future Work

7.1: Conclusions

In the investigation of phase stability in nickel superalloys, the ternary system of alloying elements Cr-Hf-Y was modeled using the CALPHAD approach. It is important to understand what phases are thermodynamically stable before processing nickel superalloys. The ternary modeling was done by first modeling the three binary systems that make up the Cr-Hf-Y system.

The Hf-Y system contains no compounds and has very limited solid solubility. First-principles calculations were done on the HCP and BCC structures by way of the Special Quasirandom Structure (SQS) method. An investigation into the symmetry of the SQS structures revealed the fully relaxed case did not maintain symmetry and was not a good representation of what the structure would look like. Multiple relaxation schemes were used to determine which would best hold the symmetry of the system. From the first-principles calculation, the enthalpy of mixing for HCP and BCC was calculated and used along with experimental data to model the HF-Y binary system.

The Cr-Y system also contains no compounds and limited solid solubility, but does have a miscibility gap in the liquid phase. The ground state of BCC chromium is antiferromagnetic and ferromagnetic for HCP. This made the first-principles calculations a bit more complex. As with Hf-Y, similar relaxation methods and symmetry investigations were performed. To deal with the antiferromagnetic chromium, multiple magnetic configurations were calculated. The

enthalpy of mixing values for the HCP and BCC phases were calculated and used to model the system with the aid of experimental data.

The Cr-Hf system contains three polymorphs of the Laves phase Cr_2Hf. Previous experimental work was in disagreement between which Laves phases were stable. The transition between polymorphs is sluggish, so experimentally determining the transition temperatures can be difficult. Using previously published first-principles calculations and experiments using longer anneal times, the transition temperatures of the Laves phases was modeled. This was then included in the modeling. This work found all three polymorphs were stable at different temperature range, whereas previous modeling had only one or two of the polymorph as stable. This is an important aspect of the modeling's success, as experiments were incorrect because of the slow kinetics of the transformation reaction.

The three binary systems were then combined to make the Cr-Hf-Y ternary system. This is a useful tool in determining phase stability in nickel superalloys. While this ternary system may be modeled, there is still additional work to be done.

7.2: Future Work

- Improve the quality of the modeling with new data:
  - Perform ternary first-principles calculations on BCC and HCP phases for enthalpy of mixing data
  - Calculations for the solubility of the Laves phases
  - Improve magnetic calculations
  - Finite temperature properties of the Laves phases
- Incorporate ternary experiments into the modeling work
- Integration into the nickel superalloy database

Appendix A

Pure Element First-Principles Calculations

This appendix contains first-principles calculations of the pure elements. For each structure, the calculations done in this work are compared to previously published first-principles work and published experiments. Both total energy per atom and lattice parameter values are listed.

Table A.1: First-principles calculations of BCC and HCP hafnium compared to published first-principles calculations and experimental lattice parameters

		Total Energy		Lattice Parameter (Å)			
		(eV/atom)	% Difference	a	% Difference	c/a	% Difference
BCC	This Work	-9.7035	0.49%	3.530			
	F-P[30]	-9.6562		3.538	-0.23%		
	Exp[31]			3.615	-2.35%		
HCP	This Work	-9.8769	0.46%	3.193		1.581	
	F-P [30]	-9.8320		3.200	-0.22%	1.580	0.08%
	Exp[31]			3.195	-0.05%	1.581	0.01%

Table A.2: First-principles calculations of BCC and HCP yttrium compared to published first-principles calculations and experimental lattice parameters

		Total Energy		Lattice Parameter (Å)			
		(eV/atom)	% Difference	a	% Difference	c/a	% Difference
BCC	This Work	-6.2565	-0.02%	4.014			
	F-P[30]	-6.2577		4.029	-0.38%		
	Exp[32]			4.100	-2.11%		
HCP	This Work	-6.3797	-0.06%	3.631		1.552	
	F-P[30]	-6.3836		3.654	-0.62%	1.546	0.40%
	Exp[32]			3.643	-0.32%	1.573	-1.33%

Table A.3: First-principles calculations of BCC and HCP chromium compared to published first-principles calculations and experimental lattice parameters

		Total Energy (eV/atom)	% Difference	Lattice Parameter (Å) a	% Difference	c/a	% Difference
BCC	This Work	-9.5240	0.62%	2.842			
	F-P[30]	-9.4655		2.847	-0.19%		
	Exp[31]			2.885	-1.49%		
HCP	This Work	-9.0696	-0.06%	2.471		1.801	
	F-P[30]	-9.0751		2.485	-0.57%	1.786	0.86%

Appendix B

Isothermal Sections of the Ternary Phase Diagram

This appendix contains isothermal sections of the Cr-Hf-Y system. The evolution of ternary phase stability during cooling can be seen through the decreasing temperature sections.

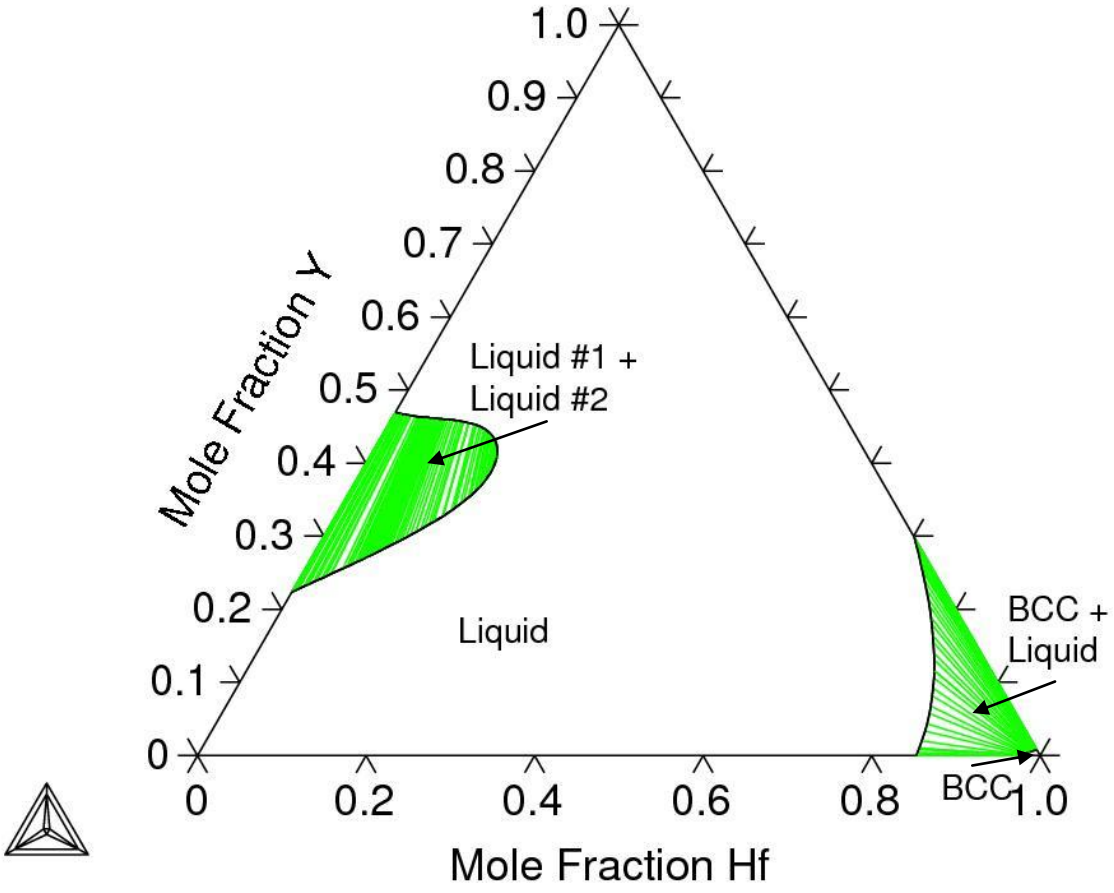

Figure B-1: Isothermal section of the Cr-Hf-Y system at 2200 K

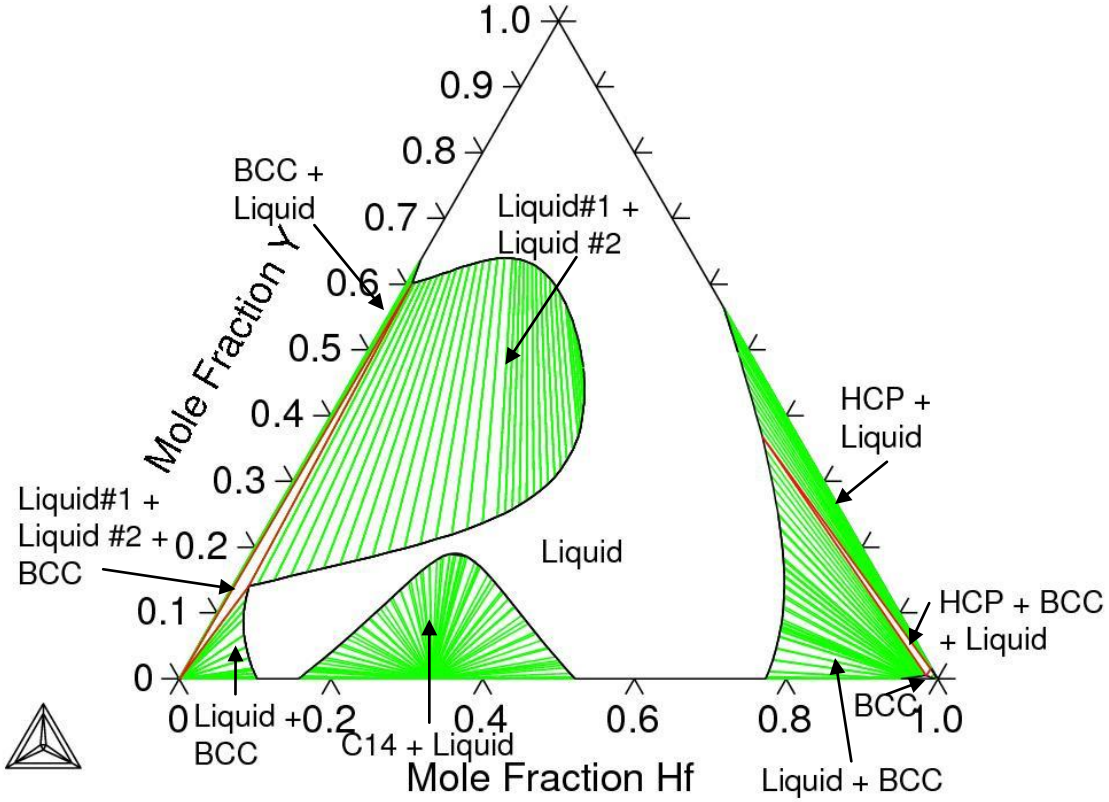

Figure B-2: Isothermal section of the Cr-Hf-Y system at 2000 K

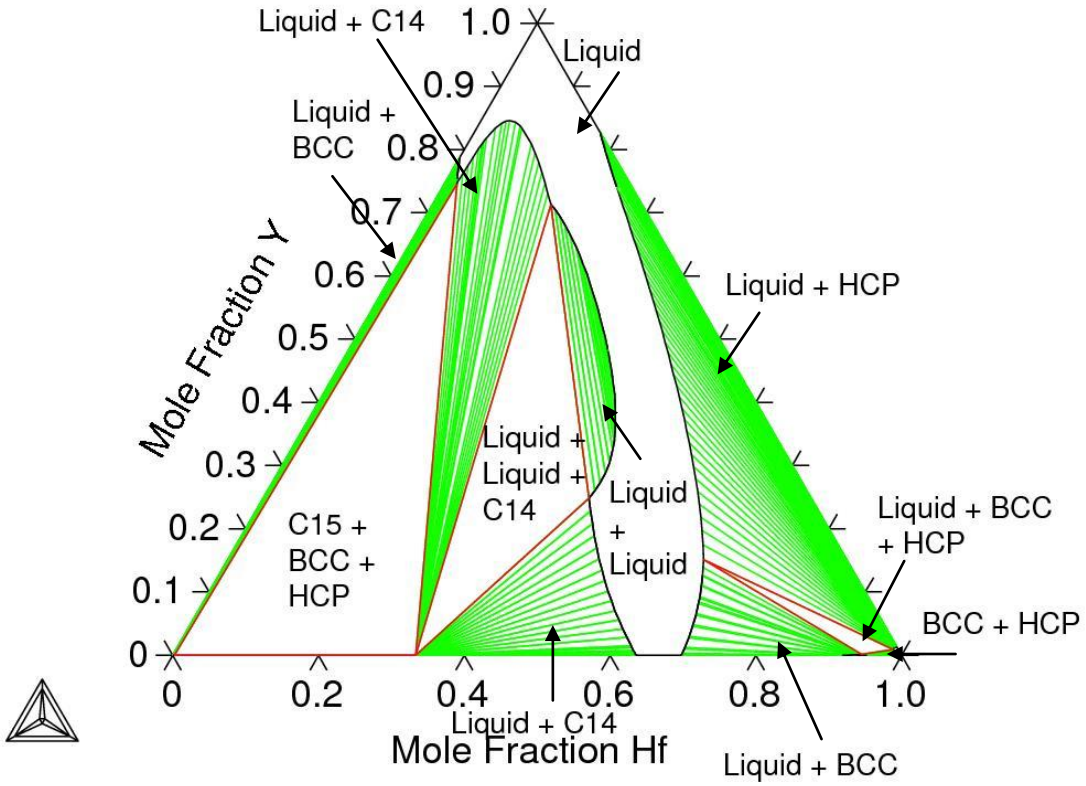

Figure B-3: Isothermal section of the Cr-Hf-Y system at 1800 K

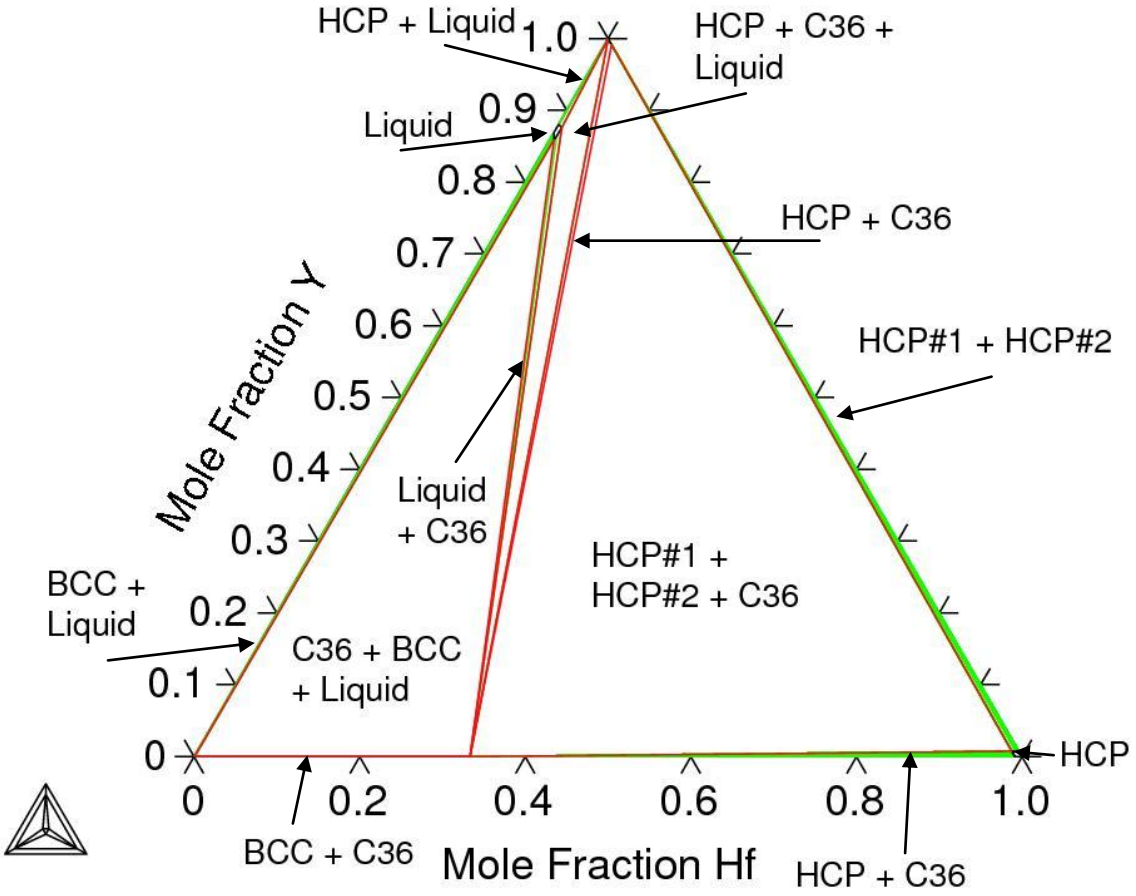

Figure B-4: Isothermal section of the Cr-Hf-Y system at 1600 K

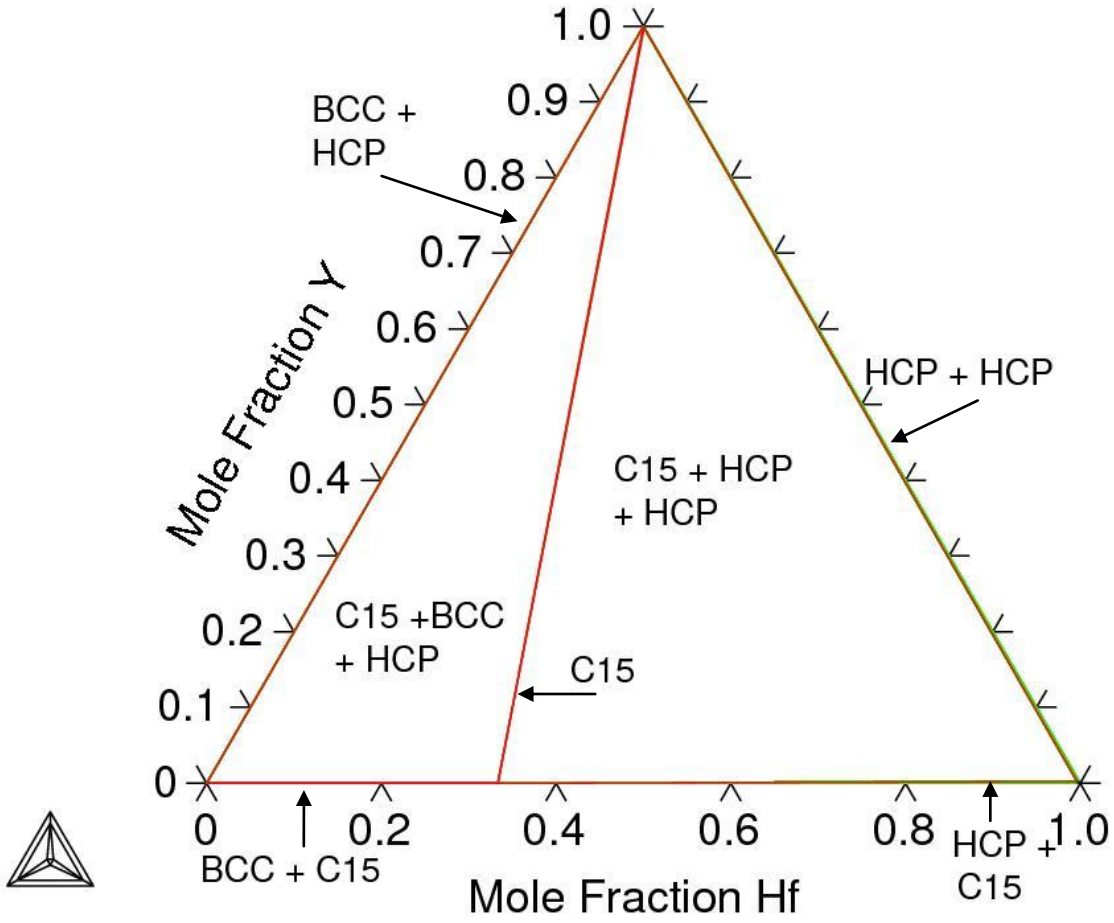

Figure B-5: Isothermal section of the Cr-Hf-Y system at 1273 K

Appendix C

Thermo-Calc Database

```
ELEMENT /-   ELECTRON_GAS              0.0000E+00  0.0000E+00  0.0000E+00!
 ELEMENT VA   VACUUM                   0.0000E+00  0.0000E+00  0.0000E+00!
 ELEMENT CR   BCC_A2                   5.1996E+01  4.0500E+03  2.3560E+01!
 ELEMENT HF   HCP_A3                   1.7849E+02  0.0000E+00  0.0000E+00!
 ELEMENT Y    HCP_A3                   8.8906E+01  0.0000E+00  0.0000E+00!


 FUNCTION GHSERCR    2.98140E+02  -8856.94+157.48*T-26.908*T*LN(T)
    +.00189435*T**2-1.47721E-06*T**3+139250*T**(-1);  2.18000E+03  Y
     -34869.344+344.18*T-50*T*LN(T)-2.88526E+32*T**(-9);  6.00000E+03  N !
 FUNCTION GHSERHF    2.98140E+02  -6987.297+110.744026*T-22.7075*T*LN(T)
    -.004146145*T**2-4.77E-10*T**3-22590*T**(-1);  2.50600E+03  Y
     -1446776.33+6193.60999*T-787.536383*T*LN(T)+.1735215*T**2
    -7.575759E-06*T**3+5.01742495E+08*T**(-1);  3.00000E+03  N !
 FUNCTION CRHFV10    2.98150E+02  -20000;   6.00000E+03   N !
 FUNCTION CRHFV11    298.15 0.0; 6000.00  N !
 FUNCTION CRHFV12    2.98150E+02  6000;   6.00000E+03   N !
 FUNCTION CRHFV13    298.15 0.0; 6000.00  N !
 FUNCTION CRHFV20    2.98150E+02  20000;   6.00000E+03   N !
 FUNCTION CRHFV21    2.98150E+02  6;   6.00000E+03   N !
 FUNCTION CRHFV22    2.98150E+02  30000;   6.00000E+03   N !
 FUNCTION CRHFV23    2.98150E+02  -5.5;   6.00000E+03   N !
 FUNCTION CRHFV5     2.98150E+02  -29600;   6.00000E+03   N !
 FUNCTION CRHFV6     2.98150E+02  -5.5;   6.00000E+03   N !
 FUNCTION CRHFV1     2.98150E+02  -34900;   6.00000E+03   N !
 FUNCTION CRHFV2     2.98150E+02  -2.07;   6.00000E+03   N !
 FUNCTION CRHFV3     2.98150E+02  -32500;   6.00000E+03   N !
 FUNCTION CRHFV4     2.98150E+02  -3.7;   6.00000E+03   N !
 FUNCTION CRHFV30    2.98150E+02  30000;   6.00000E+03   N !
 FUNCTION CRHFV31    298.15 0.0; 6000.00  N !
 FUNCTION CRHFV32    2.98150E+02  -10000;   6.00000E+03   N !
 FUNCTION CRHFV33    298.15 0.0; 6000.00  N !
 FUNCTION CRYV1      2.98150E+02  32481.1569;   6.00000E+03   N !
 FUNCTION CRYV2      298.15 0.0; 6000.00  N !
 FUNCTION CRYV3      2.98150E+02  10065.7284;   6.00000E+03   N !
 FUNCTION CRYV4      298.15 0.0; 6000.00  N !
 FUNCTION CRYV5      298.15 0.0; 6000.00  N !
 FUNCTION CRYV6      298.15 0.0; 6000.00  N !
 FUNCTION CRYV20     2.98150E+02  300000;   6.00000E+03   N !
 FUNCTION CRYV21     298.15 0.0; 6000.00  N !
 FUNCTION CRYV22     2.98150E+02  230000;   6.00000E+03   N !
 FUNCTION CRYV23     298.15 0.0; 6000.00  N !
```

```
FUNCTION CRYV24     298.15 0.0; 6000.00  N !
FUNCTION CRYV25     298.15 0.0; 6000.00  N !
FUNCTION GHSERYY    1.00000E+02  -8011.09379+128.572856*T
   -25.6656992*T*LN(T)-.00175716414*T**2-4.17561786E-07*T**3
   +26911.509*T**(-1);  1.00000E+03  Y
    -7179.74574+114.497104*T-23.4941827*T*LN(T)-.0038211802*T**2
   -8.2534534E-08*T**3;  1.79515E+03  Y
    -67480.7761+382.124727*T-56.9527111*T*LN(T)+.00231774379*T**2
   -7.22513088E-08*T**3+18077162.6*T**(-1);  3.70000E+03  N !
FUNCTION CRYV10     2.98150E+02  260000;   6.00000E+03   N !
FUNCTION CRYV11     298.15 0.0; 6000.00  N !
FUNCTION CRYV12     2.98150E+02  150000;   6.00000E+03   N !
FUNCTION CRYV13     298.15 0.0; 6000.00  N !
FUNCTION CRYV14     298.15 0.0; 6000.00  N !
FUNCTION CRYV15     298.15 0.0; 6000.00  N !
FUNCTION HFYV1      2.98150E+02  4781.666;   6.00000E+03   N !
FUNCTION HFYV2      2.98150E+02  12.161926;   6.00000E+03   N !
FUNCTION HFYV3      2.98150E+02  -1975.23314;   6.00000E+03   N !
FUNCTION HFYV4      298.15 0.0; 6000.00  N !
FUNCTION HFYV5      2.98150E+02  5756.55917;   6.00000E+03   N !
FUNCTION HFYV6      298.15 0.0; 6000.00  N !
FUNCTION HFYV11     2.98150E+02  79516.7059;   6.00000E+03   N !
FUNCTION HFYV12     298.15 0.0; 6000.00  N !
FUNCTION HFYV13     298.15 0.0; 6000.00  N !
FUNCTION HFYV14     298.15 0.0; 6000.00  N !
FUNCTION HFYV15     298.15 0.0; 6000.00  N !
FUNCTION HFYV16     298.15 0.0; 6000.00  N !
FUNCTION HFYV21     2.98150E+02  64776.4706;   6.00000E+03   N !
FUNCTION HFYV22     298.15 0.0; 6000.00  N !
FUNCTION HFYV23     298.15 0.0; 6000.00  N !
FUNCTION HFYV24     298.15 0.0; 6000.00  N !
FUNCTION HFYV25     298.15 0.0; 6000.00  N !
FUNCTION HFYV26     298.15 0.0; 6000.00  N !
FUNCTION UN_ASS 298.15 0; 300 N !

TYPE_DEFINITION % SEQ *!
DEFINE_SYSTEM_DEFAULT ELEMENT 2 !
DEFAULT_COMMAND DEF_SYS_ELEMENT VA /- !


PHASE LIQUID:L %  1  1.0  !
  CONSTITUENT LIQUID:L :CR%,HF,Y :  !

 PARAMETER G(LIQUID,CR;0)  2.98140E+02  +24339.955-11.420225*T+GHSERCR#
+2.37615E-21*T**7;  2.18000E+03  Y
 -16459.984+335.616316*T-50*T*LN(T);  6.00000E+03  N REF0 !
 PARAMETER G(LIQUID,HF;0)  2.98140E+02  +20414.959+99.790933*T
-22.7075*T*LN(T)-.004146145*T**2-4.77E-10*T**3-22590*T**(-1);  1.00000E+03
 Y
```

```
 +49731.499-149.91739*T+12.116812*T*LN(T)-.021262021*T**2
+1.376466E-06*T**3-4449699*T**(-1);  2.50600E+03  Y
 -4247.217+265.470523*T-44*T*LN(T);  3.00000E+03  N REF0 !
 PARAMETER G(LIQUID,Y;0)  1.00000E+02  +2098.50738+119.41873*T
-24.6467508*T*LN(T)-.00347023463*T**2-8.12981167E-07*T**3
+23713.7332*T**(-1);  1.00000E+03  Y
 +7386.44846+19.4520171*T-9.0681627*T*LN(T)-.0189533369*T**2
+1.7595327E-06*T**3;  1.79515E+03  Y
 -12976.5957+257.400783*T-43.0952*T*LN(T);  3.70000E+03  N REF0 !
 PARAMETER G(LIQUID,CR,HF;0)  2.98150E+02  +CRHFV10#+CRHFV11#*T;
6.00000E+03   N REF0 !
 PARAMETER G(LIQUID,CR,HF;1)  2.98150E+02  +CRHFV12#+CRHFV13#*T;
6.00000E+03   N REF0 !
 PARAMETER G(LIQUID,CR,Y;0)  2.98150E+02  +CRYV1#+CRYV2#*T;   6.00000E+03
 N REF0 !
 PARAMETER G(LIQUID,CR,Y;1)  2.98150E+02  +CRYV3#+CRYV4#*T;   6.00000E+03
 N REF0 !
 PARAMETER G(LIQUID,CR,Y;2)  2.98150E+02  +CRYV5#+CRYV6#*T;   6.00000E+03
 N REF0 !
 PARAMETER G(LIQUID,HF,Y;0)  2.98150E+02  +HFYV1#+HFYV2#*T;   6.00000E+03
 N REF0 !
 PARAMETER G(LIQUID,HF,Y;1)  2.98150E+02  +HFYV3#+HFYV4#*T;   6.00000E+03
 N REF0 !
 PARAMETER G(LIQUID,HF,Y;2)  2.98150E+02  +HFYV5#+HFYV6#*T;   6.00000E+03
 N REF0 !


TYPE_DEFINITION & GES A_P_D BCC_A2 MAGNETIC  -1.0    4.00000E-01 !
PHASE BCC_A2  %&  2 1   3 !
  CONSTITUENT BCC_A2  :CR,HF,Y : VA :  !

 PARAMETER G(BCC_A2,CR:VA;0)  2.98150E+02  +GHSERCR#;   6.00000E+03   N
REF0 !
 PARAMETER TC(BCC_A2,CR:VA;0)  2.98150E+02  -311.5;   6.00000E+03   N REF0 !
 PARAMETER BMAGN(BCC_A2,CR:VA;0)  2.98150E+02  -.008;   6.00000E+03   N
REF0 !
 PARAMETER G(BCC_A2,HF:VA;0)  2.98140E+02  +5370.703+103.836026*T
-22.8995*T*LN(T)-.004206605*T**2+8.71923E-07*T**3-22590*T**(-1)
-1.446E-10*T**4;  2.50600E+03  Y
 +1912456.77-8624.20573*T+1087.61412*T*LN(T)-.286857065*T**2
+1.3427829E-05*T**3-6.10085091E+08*T**(-1);  3.00000E+03  N REF0 !
 PARAMETER G(BCC_A2,Y:VA;0)  1.00000E+02  -833.658863+123.667346*T
-25.5832578*T*LN(T)-.00237175965*T**2+9.10372497E-09*T**3
+27340.0687*T**(-1);  1.00000E+03  Y
 -1297.79829+134.528352*T-27.3038477*T*LN(T)-5.41757644E-04*T**2
-3.05012175E-07*T**3;  1.79515E+03  Y
 +15389.4975+.981325399*T-8.88296647*T*LN(T)-.00904576576*T**2
+4.02944768E-07*T**3-2542575.96*T**(-1);  3.70000E+03  N REF0 !
 PARAMETER G(BCC_A2,CR,HF:VA;0)  2.98150E+02  +CRHFV20#+CRHFV21#*T;
```

```
 6.00000E+03   N REF0 !
  PARAMETER G(BCC_A2,CR,HF:VA;1)  2.98150E+02  +CRHFV22#+CRHFV23#*T;
 6.00000E+03   N REF0 !
  PARAMETER G(BCC_A2,CR,Y:VA;0)  2.98150E+02  +CRYV20#+CRYV21#*T;
 6.00000E+03   N REF0 !
  PARAMETER G(BCC_A2,CR,Y:VA;1)  2.98150E+02  +CRYV22#+CRYV23#*T;
 6.00000E+03   N REF0 !
  PARAMETER G(BCC_A2,CR,Y:VA;2)  2.98150E+02  +CRYV24#+CRYV25#*T;
 6.00000E+03   N REF0 !
  PARAMETER G(BCC_A2,HF,Y:VA;0)  2.98150E+02  +HFYV11#+HFYV12#*T;
 6.00000E+03   N REF0 !
  PARAMETER G(BCC_A2,HF,Y:VA;1)  2.98150E+02  +HFYV13#+HFYV14#*T;
 6.00000E+03   N REF0 !
  PARAMETER G(BCC_A2,HF,Y:VA;2)  2.98150E+02  +HFYV15#+HFYV16#*T;
 6.00000E+03   N REF0 !


 TYPE_DEFINITION ' GES A_P_D CBCC_A12 MAGNETIC  -3.0    2.80000E-01 !
 PHASE CBCC_A12  %'  2 1   1 !
   CONSTITUENT CBCC_A12  :CR : VA :  !

  PARAMETER G(CBCC_A12,CR:VA;0)  2.98150E+02  +11087+2.7196*T+GHSERCR#;
 6.00000E+03   N REF0 !


 PHASE CR  %  1  1.0  !
   CONSTITUENT CR  :CR :  !

      PARA G(CR,CR;0) 298.15 0; 6000 N!


 PHASE CR2HF_C14  %  2 1   2 !
   CONSTITUENT CR2HF_C14  :HF : CR :  !

  PARAMETER G(CR2HF_C14,HF:CR;0)  2.98140E+02
+GHSERHF#+2*GHSERCR#+CRHFV5#
 +CRHFV6#*T;  3.00000E+03  N REF0 !


 PHASE CR2HF_C15  %  2 1   2 !
   CONSTITUENT CR2HF_C15  :HF : CR :  !

  PARAMETER G(CR2HF_C15,HF:CR;0)  2.98140E+02
+GHSERHF#+2*GHSERCR#+CRHFV1#
 +CRHFV2#*T;  3.00000E+03  N REF0 !


 PHASE CR2HF_C36  %  2 1   2 !
   CONSTITUENT CR2HF_C36  :HF : CR :  !
```

```
  PARAMETER G(CR2HF_C36,HF:CR;0)  2.98140E+02
+GHSERHF#+2*GHSERCR#+CRHFV3#
 +CRHFV4#*T;  3.00000E+03  N REF0 !


PHASE CUB_A13  %  2 1   1 !
   CONSTITUENT CUB_A13  :CR : VA :  !

  PARAMETER G(CUB_A13,CR:VA;0)  2.98150E+02  +15899+.6276*T+GHSERCR#;
 6.00000E+03   N REF0 !


TYPE_DEFINITION ( GES A_P_D FCC_A1 MAGNETIC  -3.0    2.80000E-01 !
PHASE FCC_A1  %(  2 1   1 !
   CONSTITUENT FCC_A1  :CR : VA :  !

  PARAMETER G(FCC_A1,CR:VA;0)  2.98150E+02  +7284+.163*T+GHSERCR#;
 6.00000E+03   N REF0 !
  PARAMETER TC(FCC_A1,CR:VA;0)  2.98150E+02  -1109;   6.00000E+03   N REF0 !
  PARAMETER BMAGN(FCC_A1,CR:VA;0)  2.98150E+02  -2.46;   6.00000E+03   N
 REF0 !


TYPE_DEFINITION ) GES A_P_D HCP_A3 MAGNETIC  -3.0    2.80000E-01 !
PHASE HCP_A3  %)  2 1   .5 !
   CONSTITUENT HCP_A3  :CR,HF%,Y : VA% :  !

  PARAMETER G(HCP_A3,CR:VA;0)  2.98150E+02  +4438+GHSERCR#;   6.00000E+03
 N REF0 !
  PARAMETER TC(HCP_A3,CR:VA;0)  2.98150E+02  -1109;   6.00000E+03   N REF0 !
  PARAMETER BMAGN(HCP_A3,CR:VA;0)  2.98150E+02  -2.46;   6.00000E+03   N
 REF0 !
  PARAMETER G(HCP_A3,HF:VA;0)  2.98140E+02  -6987.297+110.744026*T
 -22.7075*T*LN(T)-.004146145*T**2-4.77E-10*T**3-22590*T**(-1);  2.50600E+03
  Y
  -1446776.33+6193.60999*T-787.536383*T*LN(T)+.1735215*T**2
 -7.575759E-06*T**3+5.01742495E+08*T**(-1);  3.00000E+03  N REF0 !
  PARAMETER G(HCP_A3,Y:VA;0)  1.00000E+02  -8011.09379+128.572856*T
 -25.6656992*T*LN(T)-.00175716414*T**2-4.17561786E-07*T**3
 +26911.509*T**(-1);  1.00000E+03  Y
  -7179.74574+114.497104*T-23.4941827*T*LN(T)-.0038211802*T**2
 -8.2534534E-08*T**3;  1.79515E+03  Y
  -67480.7761+382.124727*T-56.9527111*T*LN(T)+.00231774379*T**2
 -7.22513088E-08*T**3+18077162.6*T**(-1);  3.70000E+03  N REF0 !
  PARAMETER G(HCP_A3,CR,HF:VA;0)  2.98150E+02  +CRHFV30#+CRHFV31#*T;
 6.00000E+03   N REF0 !
  PARAMETER G(HCP_A3,CR,HF:VA;1)  2.98150E+02  +CRHFV32#+CRHFV33#*T;
 6.00000E+03   N REF0 !
```

```
 PARAMETER G(HCP_A3,CR,Y:VA;0)  2.98150E+02  +CRYV10#+CRYV11#*T;
6.00000E+03   N REF0 !
 PARAMETER G(HCP_A3,CR,Y:VA;1)  2.98150E+02  +CRYV12#+CRYV13#*T;
6.00000E+03   N REF0 !
 PARAMETER G(HCP_A3,CR,Y:VA;2)  2.98150E+02  +CRYV14#+CRYV15#*T;
6.00000E+03   N REF0 !
 PARAMETER G(HCP_A3,HF,Y:VA;0)  2.98150E+02  +HFYV21#+HFYV22#*T;
6.00000E+03   N REF0 !
 PARAMETER G(HCP_A3,HF,Y:VA;1)  2.98150E+02  +HFYV23#+HFYV24#*T;
6.00000E+03   N REF0 !
 PARAMETER G(HCP_A3,HF,Y:VA;2)  2.98150E+02  +HFYV25#+HFYV26#*T;
6.00000E+03   N REF0 !


PHASE LAVES_C15  %  2 2   1 !
  CONSTITUENT LAVES_C15  :CR : CR :  !

 PARAMETER G(LAVES_C15,CR:CR;0)  2.98140E+02  -11570.82+472.44*T
-80.724*T*LN(T)+.00568305*T**2-4.43163E-06*T**3+417750*T**(-1);
2.18000E+03  Y
 -89608.032+1032.54*T-150*T*LN(T)-8.65578E+32*T**(-9);  6.00000E+03  N
REF0 !


PHASE Y  %  1  1.0  !
  CONSTITUENT Y  :Y :  !

    PARA G(Y,Y;0) 298.15 0; 6000 N!

LIST_OF_REFERENCES
NUMBER  SOURCE
!
```

Appendix D

Binary .pop Files

D.1: Hf-Y Binary System .pop File

```
$============================================================$
$************************************************************$
$            POP file for Hf-Y binary system                 $
$************************************************************$
$============================================================$
$                2009-8-28 Brad Hasek                        $
$============================================================$


$************************************************************$
$           Eutectic: L  <-> HCP + HCP#2                     $
$************************************************************$
create 1,1
c-s ph HCP HCP#2 liq=f 1
s-c p=1e5
exper x(liq,Y)=.879:.001
exper T=1698:1
exper x(HCP,Y)=.05:.001
exper x(HCP#2,Y)=.99:.001


$************************************************************$
$           Liquidus: L  <-> L + BCC                         $
$************************************************************$
TABLE_HEAD 100

CREATE_NEW_EQUILIBRIUM @@,1

CHANGE_STATUS PHASE BCC LIQUID=FIXED 1

SET-CONDITION P=101325, T=@3:.1
EXPERIMENT X(Liq,Y)=@1:0.005
EXPERIMENT X(BCC,Y)=@2:0.005

LABEL ALI
```

```
TABLE_VALUES

$x(Liq,Y) x(BCC,y)   T(K)

0.4         0.0025     2200
TABLE_END



$**********************************************************************$
$            Liquidus: L  <-> L + HCP                    $
$**********************************************************************$
TABLE_HEAD 200

CREATE_NEW_EQUILIBRIUM @@,1

CHANGE_STATUS PHASE HCP LIQUID=FIXED 1

SET-CONDITION P=101325, T=@3:0
EXPERIMENT X(Liq,Y)=@1:0.005

EXPERIMENT X(HCP,Y)=@2:0.005

LABEL ALI

TABLE_VALUES

$x(Liq,Y) x(HCP,y)   T(K)

0.70     0.01       1900

$TABLE_END

$**********************************************************************$
$======================================================================$
$**********************************************************************$
$                      BCC- SQS                      $
$                   Assessed for BCC-A2                    $
$                                        $
$**********************************************************************$
$======================================================================$
TABLE_HEAD 1000

CREATE_NEW_EQUILIBRIUM @@,1

CHANGE_STATUS PHASE BCC_A2=FIXED 1

SET_REFERENCE_STATE HF BCC_A2,,,
```

```
SET_REFERENCE_STATE Y BCC_A2,,,

SET-CONDITION P=101325  T=298.15  X(BCC_A2,Y)=@1

EXPERIMENT HMR=@2:1000

LABEL AHMF

TABLE_VALUES

0.25 14646
0.5  19933
0.75 15101

TABLE_END

$*********************************************************************$
$=====================================================================$
$*********************************************************************$
$                    HCP- SQS                    $
$                 Assessed for HCP-A3                $
$                                  $
$*********************************************************************$
$=====================================================================$
TABLE_HEAD 2000

CREATE_NEW_EQUILIBRIUM @@,1

CHANGE_STATUS PHASE HCP_A3=FIXED 1

SET_REFERENCE_STATE HF HCP_A3,,,

SET_REFERENCE_STATE Y HCP_A3,,,

SET-CONDITION P=101325  T=298.15  X(HCP_A3,Y)=@1

EXPERIMENT HMR=@2:1000

LABEL AHMF

TABLE_VALUES

0.25 11000
0.5  16570
0.75 12790
TABLE_END
save
```

D.2: Cr-Y Binary System .pop File

```
$=========================================================$
$*********************************************************$
$            POP file for Cr-Y binary system              $
$*********************************************************$
$=========================================================$
$                2009-10-20 Brad Hasek                    $
$=========================================================$

$=========================================================$
$            Two Eutectic from 1961 Ter                   $
$=========================================================$

$=========================================================$


$*********************************************************$
$            Eutectic: L  <-> HCP + BCC                   $
$*********************************************************$
create 1,1
c-s ph BCC HCP liq=f 1
s-c p=1e5
exper x(liq,Y)=.859:.001 T=1573:5
exper x(hcp,y)=.999:.001 T=1573:5
exper x(bcc,y)=.005:.001 T=1573:5

$*********************************************************$
$            Eutectic: L#1  <-> L#2 + BCC                 $
$*********************************************************$
create 2,1
c-s ph BCC liq#1 liq#2=f 1
s-c p=1e5
exper x(liq#2,y)=.0936:.001 T=2033:5
exper x(bcc,y)=.002:.001 T=2033:5
exper x(liq#1,y)=.577:.001 T=2033:5



$*********************************************************$
$           Eutectiod: BCC Y <-> L + HCP Y                $
$*********************************************************$
create 3,1
c-s ph BCC liq HCP=f 1
s-c p=1e5
exper x(BCC,y)=.99:.001 T=1781:5
exper x(hcp,y)=.999:.001 T=1781:5
exper x(liq,y)=.981:.001 T=1781:5
```

```
$*********************************************************************$
$*********************************************************************$
$                PART. I Thermochemical data                 $
$*********************************************************************$
$*********************************************************************$

$=============================================================$

$*********************************************************************$
$                     BCC- SQS                      $
$                  Assessed for BCC-A2                   $
$                                        $
$*********************************************************************$

$=============================================================$
TABLE_HEAD 1000

CREATE_NEW_EQUILIBRIUM @@,1

CHANGE_STATUS PHASE BCC=FIXED 1

SET_REFERENCE_STATE Cr BCC,,,

SET_REFERENCE_STATE Y BCC,,,

SET-C P=101325 T=298.15 X(BCC,Y)=@1
EXPERIMENT HMR=@2:1000

LABEL AHMF

TABLE_VALUES
0.25  83590
0.5   62360
0.75  31200

TABLE_END
```

```
$============================================================$

$************************************************************$
$                    HCP- SQS                    $
$                 Assessed for HCP                  $
$                                        $
$************************************************************$

$============================================================$
TABLE_HEAD 2000

CREATE_NEW_EQUILIBRIUM @@,1

CHANGE_STATUS PHASE HCP=FIXED 1

SET_REFERENCE_STATE Cr HCP,,,

SET_REFERENCE_STATE Y HCP,,,

SET-C P=101325 T=298.15 X(HCP,Y)=@1
EXPERIMENT HMR=@2:1000

LABEL AHMF

TABLE_VALUES
0.25  71082
0.5   52720
0.75  27626


TABLE_END

save
```

D.3: Cr-Hf Binary System .pop File

```
$$$$$$$$$$$$$$$$$$$$
$$ SVENCHNIKOV 1965
$$$$$$$$$$$$$$$$$$$$

$$ LIQUIDUS CR
TABLE 100
CREATE-NEW-EQUILIBRIUM @@,1
CHANGE-STATUS PHASES LIQUID BCC=FIXED 1
SET-CONDITION P=1E5 X(LIQUID,CR)=@1
EXPERIMENT T=@2:10
TABLE-VALUES
0.8956 1923
0.9214 1977
0.9469 1991
0.9796 2027
TABLE-END

$$ CONGRUENT MELTING
CREATE 1,1
CHANGE-STATUS PHASES LIQUID CR2HF_C14=FIXED 1
SET-CONDITION P=1E5 3*X(LIQUID,CR)=1
EXPERIMENT T=2074:10

$$ LIQUIDUS C14
TABLE 200
CREATE-NEW-EQUILIBRIUM @@,1
CHANGE-STATUS PHASES LIQUID CR2HF_C14=FIXED 1
SET-CONDITION P=1E5 X(LIQUID,CR)=@1
EXPERIMENT T=@2:10
TABLE-VALUES
0.3015 1692
0.4015 1861
0.5027 1980
0.6049 2051
0.7012 2063
0.7998 1988
0.8448 1944
TABLE-END

$$ LIQUIDUS HF
TABLE 300
CREATE-NEW-EQUILIBRIUM @@,1
CHANGE-STATUS PHASES LIQUID BCC=FIXED 1
SET-CONDITION P=1E5 X(LIQUID,CR)=@1
EXPERIMENT T=@2:10
TABLE-VALUES
```

```
0.0746 2073
0.1026 2011
0.1500 1901
0.2030 1772
TABLE-END

$$ EUTECTOID HF
CREATE 2,1
CHANGE-STATUS PHASES BCC HCP CR2HF_C14=FIXED 1
SET-CONDITION P=1E5
EXPERIMENT X(BCC,CR)=0.0732:0.001 T=1594:10



$$$$$$$$$$$$$$$$$$$
$$ CARLSON 1968
$$$$$$$$$$$$$$$$$$$

$$ LIUQIDUS CR
TABLE 400
CREATE-NEW-EQUILIBRIUM @@,1
CHANGE-STATUS PHASES LIQUID BCC=FIXED 1
SET-CONDITION P=1E5 X(LIQUID,CR)=@1
EXPERIMENT T=@2:10
TABLE-VALUES
0.9214 2037
0.9324 2098
TABLE-END

$$ EUTECTIC CR
CREATE 3,1
CHANGE-STATUS PHASES BCC LIQUID CR2HF_C14=FIXED 1
SET-CONDITION P=1E5
EXPERIMENT X(BCC,CR)=0.8520:0.001 T=1940:10

$$ CONGRUENT MELTING
create 4,1
CHANGE-STATUS PHASES LIQUID CR2HF_C14=FIXED 1
SET-CONDITION P=1E5 3*X(LIQUID,CR)=1
EXPERIMENT T=2110:10

$$ EUTECTIC HF
TABLE 500
CREATE-NEW-EQUILIBRIUM @@,1
CHANGE-STATUS PHASES LIQUID BCC CR2HF_C14=FIXED 1
SET-CONDITION P=1E5
EXPERIMENT X(LIQUID,CR)=@1:0.001 T=@2:10
TABLE-VALUES
0.2983 1753
```

```
0.2898 1734
0.3141 1727
TABLE-END

$$ SOLIDUS HF
TABLE 600
CREATE-NEW-EQUILIBRIUM @@,1
CHANGE-STATUS PHASES LIQUID BCC=FIXED 1
SET-CONDITION P=1E5 X(BCC,CR)=@1
EXPERIMENT T=@2:10
TABLE-VALUES
0.0287 2441
0.0652 2305
0.0652 2262
0.1016 2158
0.1441 1955
TABLE-END

$$ SOLVUS HF
TABLE 700
CREATE-NEW-EQUILIBRIUM @@,1
CHANGE-STATUS PHASES HCP BCC=FIXED 1
SET-CONDITION P=1E5 X(HCP,CR)=@1
EXPERIMENT T=@2:10
TABLE-VALUES
0.0199 1945
0.0369 1918
0.0393 1943
0.0600 1911
TABLE-END



$$$$$$$$$$$$$$$$$$$
$$ RUDY 1968
$$$$$$$$$$$$$$$$$$$

$$ EUTECTIC CR
CREATE 5,1
CHANGE-STATUS PHASES BCC LIQUID CR2HF_C14=FIXED 1
SET-CONDITION P=1E5
EXPERIMENT X(BCC,CR)=0.8768:0.001 T=1977:10

$$ CONGRUENT MELTING
TABLE 800
CREATE-NEW-EQUILIBRIUM @@,1
CHANGE-STATUS PHASES LIQUID CR2HF_C14=FIXED 1
SET-CONDITION P=1E5 3*X(LIQUID,CR)=1
EXPERIMENT T=@1:10
```

```
TABLE-VALUES
2153
2140
TABLE-END

$$ EUTECTIC HF
CREATE 6,1
CHANGE-STATUS PHASES BCC LIQUID CR2HF_C14=FIXED 1
SET-CONDITION P=1E5
EXPERIMENT X(BCC,CR)=0.4033:0.001 T=1789:10

$$ SOLIDUS HF
TABLE 900
CREATE-NEW-EQUILIBRIUM @@,1
CHANGE-STATUS PHASES LIQUID BCC=FIXED 1
SET-CONDITION P=1E5 X(BCC,CR)=@1
EXPERIMENT T=@2:10
TABLE-VALUES
0.0533 2331
0.1030 2076
TABLE-END

$$ EUTECTOID HF
TABLE 1000
CREATE-NEW-EQUILIBRIUM @@,1
CHANGE-STATUS PHASES BCC HCP CR2HF_C14=FIXED 1
SET-CONDITION P=1E5
EXPERIMENT X(BCC,CR)=@1:0.001 T=@2:10
TABLE-VALUES
0.1049 1644
0.1049 1626
TABLE-END

$$ SOLVUS HF
TABLE 1100
CREATE-NEW-EQUILIBRIUM @@,1
CHANGE-STATUS PHASES HCP BCC=FIXED 1
SET-CONDITION P=1E5 X(HCP,CR)=@1
EXPERIMENT T=@2:10
TABLE-VALUES
0.0355  1952
0.0613  1875
0.0807  1779
0.1039  1680
TABLE-END
```

```
$$ STABILITY CONDITIONS
CREATE 7,1
CHANGE-STATUS PHASES CR2HF_C14 BCC=ENTERED 1
SET-CONDITION P=1E5 T=1700 X(CR)=0.95 N=1
EXPERIMENT X(BCC,CR)=0.995:0.005

SAVE
```

Bibliography

1. Hohenberg, P. and W. Kohn, *Inhomogeneous Electron Gas.* Physical Review B, 1964. **136**(3B): p. B864-&.
2. Kohn, W. and L.J. Sham, *Self-Consistent Equations Including Exchange and Correlation Effects.* Physical Review, 1965. **140**(4A): p. 1133-&.
3. Ceperley, D.M. and B.J. Alder, *Ground-State of the Electron-Gas by a Stochastic Method.* Physical Review Letters, 1980. **45**(7): p. 566-569.
4. Perdew, J.P., K. Burke, and Y. Wang, *Generalized Gradient Approximation for the Exchange-Correlation Hole of a Many-Electron System.* Physical Review B, 1996. **54**(23): p. 16533-16539.
5. Soven, P., *Coherent-Potential Model of Substitutional Disordered Alloys.* Physical Review, 1967. **156**(3): p. 809-&.
6. Kissavos, A.E., et al., *A Critical Test of Ab Initio and Calphad Methods: The Structural Energy Difference between Bcc and Hcp Molybdenum.* Calphad-Computer Coupling of Phase Diagrams and Thermochemistry, 2005. **29**(1): p. 17-23.
7. Lu, Z.W., S.H. Wei, and A. Zunger, *Large Lattice-Relaxation-Induced Electronic Level Shifts in Random Cu1-Xpdx Alloys.* Physical Review B, 1991. **44**(7): p. 3387-3390.
8. Sanchez, J.M., *Cluster Expansions and the Configurational Energy of Alloys.* Physical Review B, 1993. **48**(18): p. 14013-14015.
9. Zunger, A., et al., *Special Quasirandom Structures.* Physical Review Letters, 1990. **65**(3): p. 353-356.
10. Redlich, O. and A.T. Kister, *Algebraic Representation of Thermodynamic Properties and the Classification of Solutions.* Industrial and Engineering Chemistry, 1948. **40**(2): p. 345-348.
11. Perdew, J.P., et al., *Atoms, Molecules, Solids, and Surfaces - Applications of the Generalized Gradient Approximation for Exchange and Correlation.* Physical Review B, 1992. **46**(11): p. 6671-6687.
12. Lundin, C.E. and D.T. Klodt, *Phase Equilibria of Group 4a Metals with Yttrium.* Transactions of the Metallurgical Society of Aime, 1962. **224**(2): p. 367-&.
13. Jiang, C., et al., *First-Principles Study of Binary Bcc Alloys Using Special Quasirandom Structures.* Physical Review B, 2004. **69**(21): p. 214202.
14. Shin, D., et al., *Thermodynamic Properties of Binary Hcp Solution Phases from Special Quasirandom Structures.* Physical Review B, 2006. **74**(2): p. 024204.
15. Terekhova, V.F., I.A. Markova, and E.M. Savitskii, *Diagramma Sostoyaniya Splavov Sistemy Khrom-Ittrii.* Zhurnal Neorganicheskoi Khimii, 1961. **6**(5): p. 1252-&.
16. Venkatraman, M., *The Cr-Y (Chromium - Yttrium) System.* Bull. Alloy Phase Diagrams, 1985. **6**(5): p. 429-431.
17. Okamoto, H., *Cr-Y (Chromium - Yttrium).* Journal of Phase Equilibria, 1992. **13**(1): p. 100-101.
18. Okamoto, H., *Thermodynamically Improbable Phase Diagrams.* Journal of Phase Equilibria, 1991. **12**(2): p. 148-168.
19. Chan, W., et al., *Thermodynamic Assessment of Cr-Rare Earth Systems.* Journal of Phase Equilibria and Diffusion, 2009. **30**(6): p. 578-586.
20. Goniakowski, J. and M. Podgorny, *Antiferromagnetism in Hexagonal Chromium, Manganese, and Iron.* Physical Review B, 1991. **44**(22): p. 12348-12352.
21. Moruzzi, V.L. and P.M. Marcus, *Antiferromagnetic Ground-State of Bcc Chromium.* Physical Review B, 1992. **46**(5): p. 3171-3174.

22. Yang, Y., et al., *Thermodynamic Modeling of the Cr-Hf-Si System.* Intermetallics, 2009. **17**(5): p. 305-312.
23. Carlson, O.N. and Alexande.Dg, *Hafnium-Chromium System.* Journal of the Less-Common Metals, 1968. **15**(4): p. 361-&.
24. Svechnikov, V.N., Shurin, A.K., Dmitrieva, G.P., and Prevrashchen, F., *V Metal. I Splavakh (Phase Conversions in Metals and Alloys).* Akad Nauk Ukr SSR 1965: p. 159-162.
25. Rudy, E. and S. Windisch, *Phase Diagrams Hafnium-Vanadium and Hafnium-Chromium.* Journal of the Less-Common Metals, 1968. **15**(1): p. 13-&.
26. Venkatraman, M.a.N., J, *The Cr-Hf (Chromium-Hafnium) System.* Bull. Alloy Phase Diagrams, 1986. **7**(6): p. 570-573.
27. Minayeva, S.A. and P.B. Budberg, *Phase-Equilibria in V-Hf-Cr System.* Russian Metallurgy, 1975(3): p. 179-182.
28. Minayeva, S.A., P.B. Budberg, and Y.K. Kovneristyy, *Phase-Structure of V-Hf-Cr Alloys.* Russian Metallurgy, 1983(5): p. 174-177.
29. Chen, X.Q., et al., *Ab Initio Study of Ground-State Properties of the Laves Phase Compounds Ticr2,Zrcr2, and Hfcr2.* Physical Review B, 2005. **71**(17).
30. Wang, Y., et al., *Ab Initio Lattice Stability in Comparison with Calphad Lattice Stability.* Calphad-Computer Coupling of Phase Diagrams and Thermochemistry, 2004. **28**(1): p. 79-90.
31. Tonkov, E., *Phase Transformations of Elements under High Pressure*. Vol. 4. 2005: CRC Press.
32. Gschneidner, K.A., *Yttrium*, in *ASM Handbook Vol 2*. 2002, ASM International.

ACADEMIC VITA of Bradley Hasek

Bradley Hasek
127 Windermere Dr
Valencia, PA 16059
bradhasek@gmail.com

Education:
Bachelor of Science Degree in Materials Science and Engineering,
Penn State University, Spring 2010
Master of Science Degree in Materials Science and Engineering,
Penn State University, Spring 2010
Honors in Materials Science and Engineering
Thesis Title: Thermodynamic Modeling and First-Principles Calculations of the Cr-Hf-Y Ternary System
Thesis Supervisor: Zi-Kui Liu

Related Experience:
Internship with Allegheny Ludlum
Supervisor: Mark Quigley, Alan Swanson, Jeanmarie Veltri
Summer 2007, 2008, 2009

Awards:
FeMET Award
Dean's List

Presentations:
MS&T 2009 Presentation Titled: Thermodynamic Modeling and First-Principles Calculations of the Cr-Hf-Y Ternary System